



A review of properties and fabrication techniques of fiber reinforced polymer nanocomposites subjected to simulated accidental ballistic impact

Usaid Ahmed Shakil^{a,b}, Shukur Bin Abu Hassan^{a,b,*}, Mohd Yazid Yahya^{a,b}, Mujiyono^c, Didik Nurhadiyanto^c

^a School of Mechanical Engineering, Universiti Teknologi Malaysia, 81310, Johor Bahru, Malaysia

^b Centre For Advanced Composite Materials (CACM), Universiti Teknologi Malaysia, 81310, Johor Bahru, Malaysia

^c Department of Mechanical Engineering Education, Universitas Negeri Yogyakarta, 55281, Yogyakarta, Indonesia

ARTICLE INFO

Keywords:

Ballistic impact
Nanoparticles
Energy absorption
Ballistic limit velocity
Nanocomposites

ABSTRACT

Composite structure experience ballistic or high velocity impact loading during in-flight operations owing to hail, bird and debris strike. In thin laminates, such an impact entails damage resulting from complex interplay of projectile characteristics, composite material properties and environmental conditions. Delamination resistance and energy absorption are two parameters to characterize the ballistic performance of materials in research community. As out of plane properties are controlled by matrix, its microstructural modification is the primary method through which ballistic performance of composites are sought to be improved. High specific surface area nanoparticles are now being used, for matrix modification, to induce nano-scale toughness mechanisms. This paper starts with brief outline of these mechanisms followed by summarizing nanocomposite fabrication techniques and ballistic impact performance of nanocly, graphene, carbon nanotube and other miscellaneous nanoparticle reinforced composites. Finally, it highlights unexplored areas in polymer nanocomposite research with focus on ballistic performance.

1. Introduction

Continuous fiber reinforced composites are prized as materials of construction in aircraft industry because of their high specific strength, modulus and corrosion resistant [1]. In this sector, stringent safety regulations and in-service mechanical requirements lay emphasis on reliability and durability of materials. For instance, industry must comply with fire-retardance and crashworthiness standards, and these need to be considered from material design point of view. Although, composite materials offer versatility and high degree of optimization in design, inherent weaknesses like poor out of plane properties and weaker interfaces mar the prospect of their usage in structural frame [2]. Composites are susceptible to impact damage owing to runway debris or hail strike during flight that may vary in severity depending upon the strain rate [3–6]. A report prepared by German aerospace center shows that majority of these impact events occur in 50–300 m/s range [7]. The extent of damage depends on other factors too such as: (i) projectile geometry (ii) target profile (iii) projectile mass and shape [8,9]. A characteristic failure in such cases is called delamination that drastically

decreases load bearing capacity of structure under the effect of repeated loading cycles.

Out of plane properties of these composites have been identified to be dominated by matrix properties. As the primary target of projectile is matrix, incipient defects occur in matrix that eventually retards composite's capability to transfer load to fibers. Performance critical property, here, is toughness that controls both energy absorption and delamination resistance of composites. Variety of methods have been opted to maximize the toughness of composites, predominantly through matrix modifications, including thermoplastic phases [10–13], fabric architecture [14–17] hybridization [18–22] and nanoparticle addition [23,24]. Usage of polymer nanocomposites as building block of aircraft structures, although, is in genesis stage but their potential in future aircraft structures has been realized [25]. For instance, Lockheed Martin announced replacement of wingtip fairings material with CNT reinforced epoxy for F-35 Lightning II aircraft and stated that currently there is no hurdle in incorporating these materials for structural applications except to avoid certifications [26]. Studies have been done in anticipation of such a usage to confirm the potential of fiber reinforced

* Corresponding author. Centre for Advanced Composite Materials (CACM), Universiti Teknologi Malaysia, 81310, Johor Bahru, Malaysia.
E-mail address: shukur@utm.my (S.B. Abu Hassan).

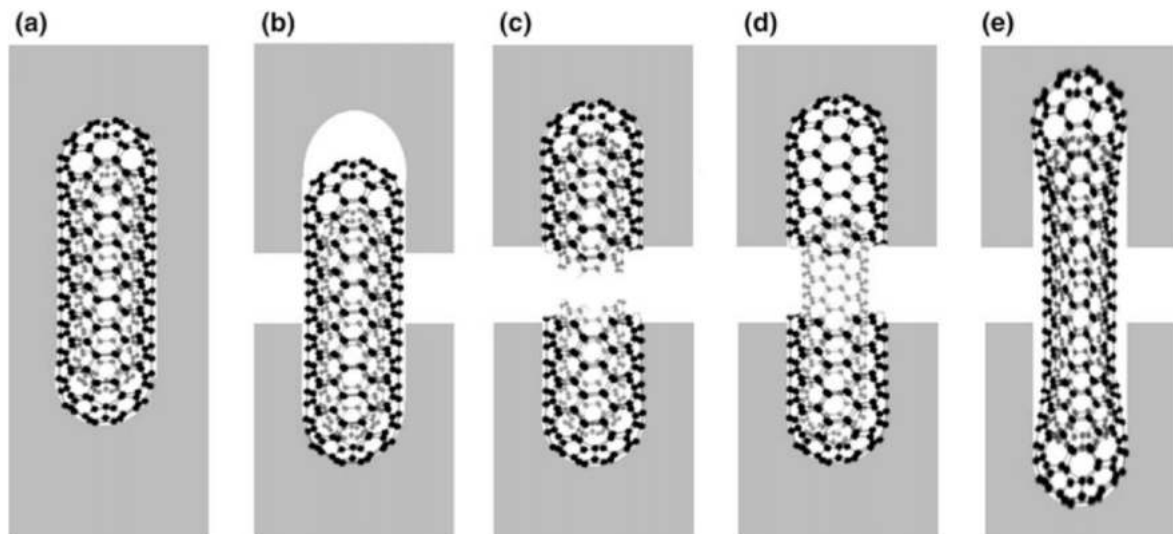


Fig. 1. (a) CNT reinforced matrix (b) CNT pull-out (c) CNT rupture (d) telescopic CNT pull-out (e) crack bridging and partial debonding of the interface [39], copyright 2005. Reproduced with permission from Elsevier Ltd.

nanocomposites in in-flight operations [27–30].

A few review paper summarize results of impact properties of composites with focus on thermoplastic matrix modifier [31], impact damage [32,33], parameters affecting impact response [34] and high-velocity properties of nanocomposites [35]. However, review of ballistic properties of nanoparticle reinforced fiber composites from the viewpoint of nanoparticle perspective is absent. This review paper presents ballistic properties of fiber reinforced thermoset composites with classification based on nanoparticle being used. With that scope, nanoparticle usage in shear thickening fluids and ceramic armors are out of reviewing activity. First part of review summarizes techniques to fabricate nanocomposites and second part presents results of studies investigating energy absorption and delamination resistance of composites tested under ballistic regime (<500 m/s). A preliminary discussion on nano-reinforcement in composites and theory of nano-scale toughness will serve to set context for advanced insights summarized in two parts of the paper. It ends with analysis of the data collected and the estimation of improvement achieved through variety of nanoparticle addition. Finally, it presents a perspective on the research theme with directions for future research endeavors.

1.1. Nanoparticle reinforcement in polymer composites

Nano-reinforcement is considered a third phase and expected to improve mechanical performance of composites. However, the mechanisms through which nano-reinforcements offer results might be completely distinct to those of micron-level reinforcement. For example, when in service load bearing efficiency of conventional micro-level reinforcement reduces, a larger surface area of nanofibers/particles may interact with matrix to offer, hitherto dormant, nano-scale responses. Another potentially insightful way to understand this phenomenon is to consider the dimension of reinforcements which are of about the same magnitude as radius of gyration of polymeric chains. Interaction of two species i.e. polymeric chains and nano-specie in a composite layer on this scale may be thought to have its own set of properties. Fig. 1 highlights various energy absorption mechanisms active in case of CNT/Epoxy composites. Some of these are discussed below to understand response of nano-particle reinforced composites.

Crack Pinning: Reinforcement acts as pinning point when encountering crack and forces crack to stretch out and produce a secondary nonlinear source. The crack stays pinned at the position of particle. For crack to propagate, an even higher energy level is required as it is related to crack length. This is called dispersion hardening which offer higher

energy absorption when finer nanoparticles are dispersed at shorter inter-particle distances.

Crack Deflection: A stiffer nano-reinforcement forces the crack to tilt or twist thereby changing the plane of propagation that in turn increases total surface area of crack. An increase in surface area increases the energy absorbed [36]. Here, hardness of nanoparticle is of utmost importance as soft particles get cut through.

Immobilized Polymer: Nanoparticle dispersed region constrains movement of polymeric chains thus requires much higher energy for chain displacement [37]. It can also alter glass transition temperature and chemical nature of composites.

Crack Bridging: It is the work done owing to nanoparticle extension over a distance within the matrix fracture plane (Fig. 1 (d)). It may contribute significantly to toughness because of high strain to failure of particles like CNT. The bridging behaviour induce nanoparticle strains that are indeed much higher than those of both the surrounding matrix and of typical micron level fibre reinforcement.

Debonding and Voids: Debonding is a widely occurring phenomenon responsible for inducing toughness in nanocomposites (Fig. 1 (e)). As crack tip is not constrained in a void, it facilitates crack growth [38]. Dissipated energy of debonding is much lower compared to other mechanisms.

1.2. Theoretical understanding of nano-scale toughness mechanism

To elucidate the effect of nano-scale reinforcement in nanocomposites, consider pull-out mechanism for both micron and nano level reinforcements. A comparison of the performance of microfiber, having critical length and given volume, with that of “n” number of nanotubes, with their critical length and total volume equivalent to that of microfiber, is appropriate [40].

Volumetric equivalence is:

$$V_{mf} = nV_{nt}$$

Where, V_{mf} and V_{nt} are volumes of micro fibre and nanotube. “n” represents number of nanotubes.

$$n = \frac{r^2 l_{mf}}{r^2 l_{nt}} \quad (1)$$

with, “r” as radius; l_{mf} and l_{nt} are critical lengths of microfiber and nanotube.

Critical length of micro and nanofiber are

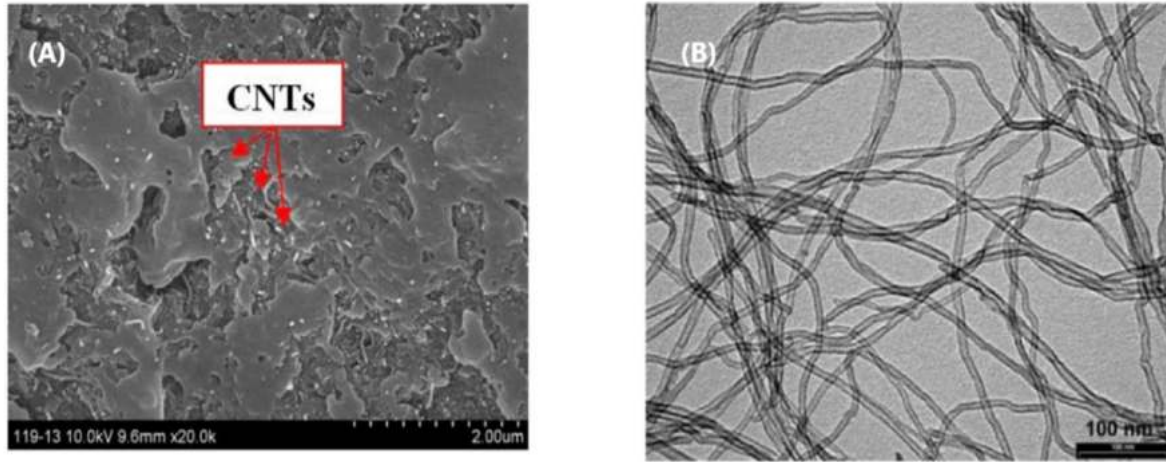


Fig. 2. (A) SEM of CNT-Epoxy composites and (B) TEM of CNT-Epoxy formulation [51], copyright 2017. Reproduced with permission from Elsevier Ltd.

$$l_{mf} = \frac{r_{mf} \sigma_{mf}}{\tau_{if, mf}}; l_{nt} = \frac{r_{nt} \sigma_{nt}}{\tau_{if, nt}} \quad (2)$$

r_{mf} and r_{nt} and radius of fiber and nanotube. σ_{mf} and $\tau_{if, mf}$ are tensile strength and interfacial strength of microfiber. σ_{nt} and $\tau_{if, nt}$ are tensile and interfacial strength of nanotube.

Noting that fiber pull-out varies over a distance 0-1/2, average value of pull-out energy per micro fibre is [41]:

$$G^f = \frac{1}{12} \pi r_f \tau_i l_c^2 \quad (3)$$

Equations (1)–(3) can be used to compare pull-out energy of microfiber to that of nanotube.

$$\frac{n G^{nt}}{G^f} = \frac{\sigma_{nt}}{\sigma_{mf}} \quad (4)$$

For instance, carbon fiber and carbon nanotube have strength of 2.5 GPa [42] and 50 GPa [43] respectively. This will offer a value of 20 for expression in equation (4). It shows the nanotube's potential as source of toughness in case of pull-out mechanism.

1.3. Nanocomposite fabrication

Fabrication of nanocomposite is a challenging task considering the enormous surface area to volume ratio of nanoparticles [44,45] that induces entanglement forces thus causing agglomeration. Deagglomeration and exfoliated structure are the two final objectives of nanocomposite fabrication attempts. Several approaches are in vogue to fabricate nanocomposites such as in-situ particle processing [46], solution mixing [47], in situ polymerization [48] and melt mixing [49]. A review of the fabrication techniques surfaced two basic routes i.e. direct mixing and solvent assisted dispersion for nanocomposite preparation. A summary of these methods, with associated parameters, is described below with discussion on advantages and disadvantages.

1.3.1. Direct mixing

Direct mixing, generally, involves addition of nanoparticles in resin or hardener and attain dispersion through mechanical agitation. Soliman et al. added functionalized MWCNT's to epoxy before doing 1.0 h long sonication at 40 °C [23]. To ensure interaction among the functional groups on the surface of the MWCNTs and the epoxy chains, mixture was stirred for 2.0 h at 80 °C. The hardener was added after cooling the resin. The fabrication of thin woven carbon fabric composites was performed using vacuum assisted hand layup technique. Rawat et al. utilized probe sonicator for 1 h to mix MWCNTs with epoxy [50]. As probe sonicator generated heat that could eventually degrade sample,

an ice-bucket was provided with. Next, hardener was poured into the MWCNT/epoxy solution and further sonication was done for 15 min. Hand layup method was used for fiber impregnation followed by vacuum bag assisted curing. Moumen et al. mixed CNT in epoxy using high shear laboratory mixer at 2000 rpm for 30 min [51]. It was followed by ultrasonic bath assisted dispersion. Then, mixture was taken to three rolls paint mill. Author concluded that at higher weight ratio (4%) of CNT, a homogeneous mixture cannot be realized through direct mixing owing to extensive agglomeration. Fig. 2 shows (a) SEM and (b) TEM micrographs of dispersion of CNT in epoxy. Vacuum infusion process was used to fabricate laminates.

Dizaji processed nanocomposites through sonication [52]. Nano-silica or nanographene were added to epoxy resin and sonication was performed for 10 min. After the mixture temperature dropped, the hardener was added. VARTM was adopted to produce GLARE laminates. Denneulin et al. incorporated MAM copolymers, with two poly (methyl methacrylate) blocks surrounding a center block of poly (butyl acrylate), with epoxy [53,54]. It has been shown that a random copolymer of methyl methacrylate (MMA) and N, N-dimethylacrylamide (DMA) can be utilized as a miscible block for the DGEBA to improve dispersion. Nanostructure is induced by strong repulsions between the side and middle blocks governed by thermodynamics. MAM in powder form was introduced to epoxy and mixed with mechanical stirrer at 290 rpm at 110 °C for a time duration of 2 h. Koricho et al. did sonication (up to 30 kJ) after direct addition of nanoclay in epoxy [55]. A 10 s/5 s: on/off pulse could prevent overheating. Mixture was then cooled at laboratory temperature for 30 min and hardener was introduced. A hand layup method was chosen to fabricate laminate with attendant de-gassing sessions. Glass fiber/Epoxy Laminates were cured in two stages: at 60 °C for 2 h and at 94 °C for 4 h.

Hossain et al. started fabrication by drying nanoclay for 2 h at 100 °C to remove moisture [56]. Nanoclay was added to epoxy and magnetically stirred for 10 h at 50–55 °C. Hardener was mixed with modified epoxy using mechanical stirrer for 5 min. System was placed in oven for 30 min to allow bubbles and volatiles to leave it. VARTM assisted fabrication was done to prepare carbon/epoxy composites. A session of 24 h curing at room temperature was followed by 5 h curing at 100 °C. Rahman et al. modified fabrication technique considering risk of nanoparticle filtration by VARTM [57]. Desired concentration of graphene/nanoclay in resin was magnetically stirred for 24 h. Solution was ultrasonicated for 20 min prior to hardener addition. Individual layers were impregnated by hand layup before VARTM to inject extra resin thus minimizing void volume. This double impregnation method helped reduce voids and filtration when higher concentrations of nanoparticles were used [58]. Author claimed to prepare nanocomposites with 0–4 wt

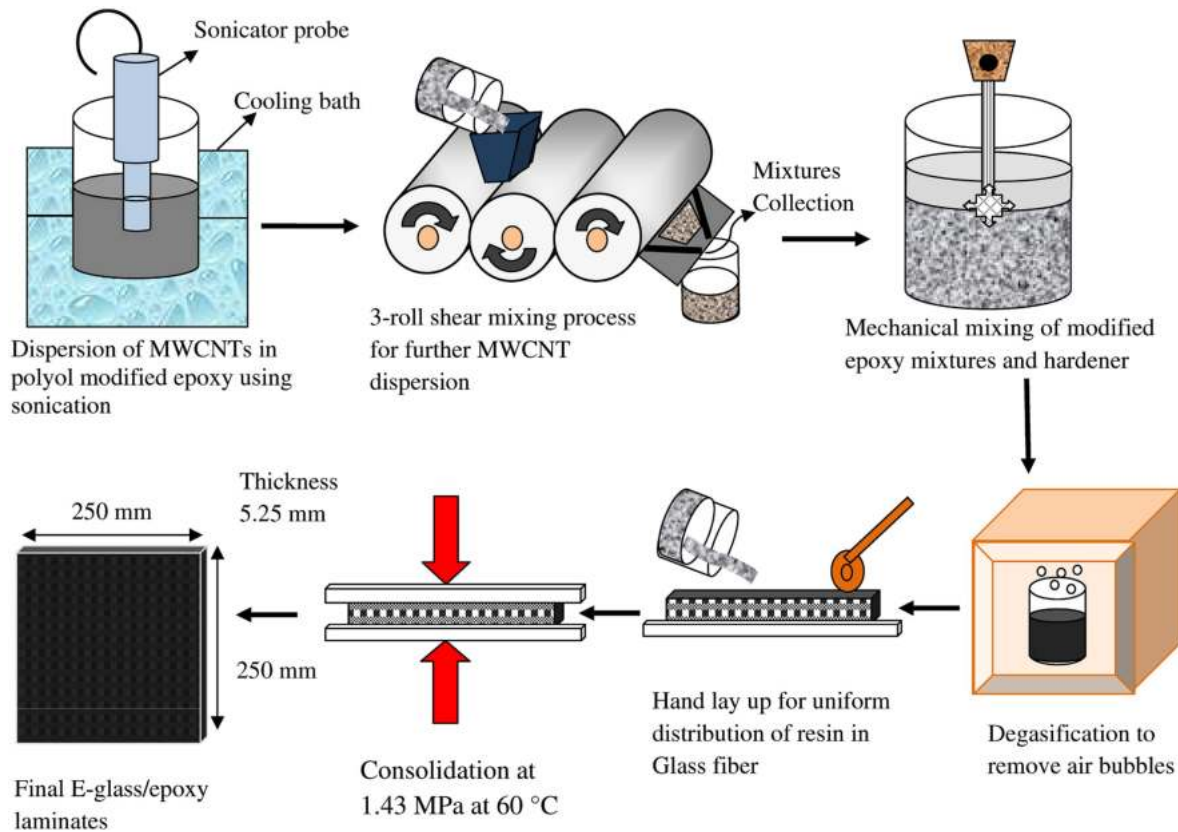


Fig. 3. Nanocomposite fabrication steps using roll-mill [63], copyright 2013. Reproduced with permission from Elsevier Ltd.

% nanoparticle concentration although with no confirmation through micrographs. Karani Dileep Kumar started with heating epoxy to 65 °C for an hour to lower viscosity of resin [59]. Resin was degassed for 20 min in vacuum oven at 65 °C. Through mechanical stirrer, operated at 500 rpm, and ultrasonication, for 20 min at 20 kHz, zinc oxide was dispersed in epoxy. Sonication time was increased with increasing concentration. Hardener was added steadily afterwards and gently agitated for 2 min prior to impregnating glass fiber. Samples were then placed in hot press for laminate curing. Landowski et al. received silica nanoparticle suspension in epoxy resin of DGEBA [60]. Mechanical stirrer helped mix base resin with silica suspension at 2800 rpm. Two degassing sessions were arranged: (i) 24 h at room temperature (ii) 24 h at 80 °C. Hardener was mixed eventually to epoxy and stirred at 1000

rpm for 1 min. Mixture was degassed for 30 min in an oven.

Rafiq et al. mixed nanoclay in epoxy using high shear mixer and degassed it for 12 h in vacuum oven under varying temperature [61]. Hardener was later added to epoxy and mixed by hand. A closed mold was utilized to cure impregnated laminates by heating it in oven. Mahdi et al. utilized functionalized MWCNT and mixed it with epoxy in desired ratio [62]. Mixture was sonicated at 40 °C, to reduce viscosity, for 30 min. Amplitude, pulse on and pulse off values were 39%, 30 s and 20 s, respectively. Compound was eventually introduced to three roll mills operated at 150 rpm. Mixture was passed three times from the mill while gradually reducing distance among rollers. Counter-rotation of successive rollers helped improve dispersion. Rahman et al. directly mixed amine functionalized MWCNT in epoxy to be sonicated (35% amplitude:

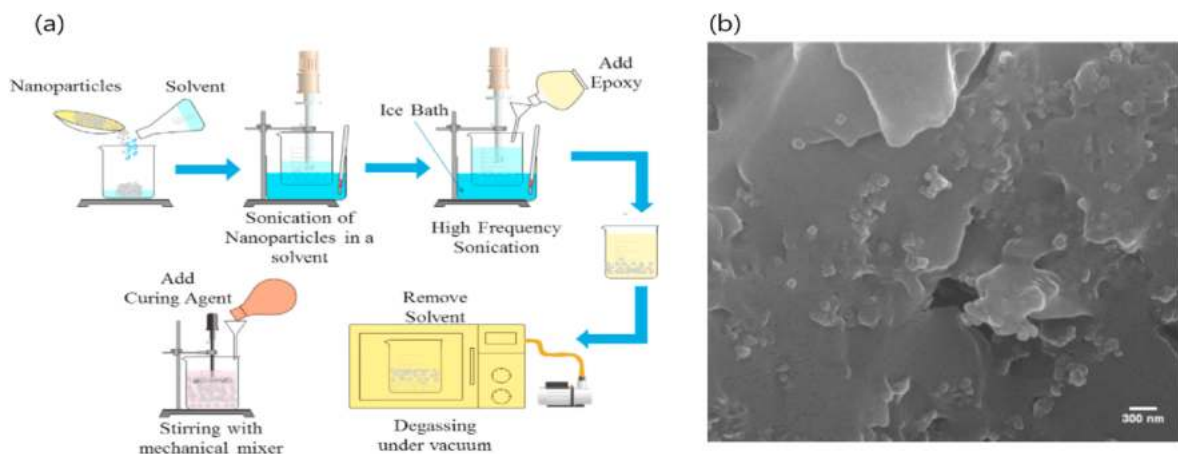


Fig. 4. (a) Process flow for alumina reinforced nanocomposite preparation (b) homogeneity at 2 wt % alumina [66], copyright 2018. Reproduced with permission from Elsevier Ltd.

Table 1
Summary of methodology opted by researchers for nanomodification of matrices.

Technique	Mechanism	Nanoparticle	Shear Mixing Time (min)	Sonication Time (min)	Additional Mechanism	Reference
Direct Mixing	Shear Forces, Cavitation-Implosion	f-MWCNT	120	60		[23]
	Cavitation-Implosion	MWCNT		60	Ice Bath	[50]
	Shear Forces, Cavitation-Implosion	CNT	30	NA	Three-roll Milling	[51]
	Cavitation-Implosion	Nanosilica/Graphene		10		[52]
	Shear Forces	MAM copolymers	90			[53,54]
	Shear Forces	Nanoclay	600		Heating (50–55 °C)	[56]
	Shear Forces, Cavitation-Implosion	Graphene/Nanoclay	30			[57]
	Shear Forces, Cavitation-Implosion	Zinc Oxide	30	20	Resin Heating	[59]
	Shear Forces, Cavitation-Implosion	f-MWCNT/Nanoclay	1440 (24h)	20	Resin Heating, Magnetic stirring	[62]
	Technique	Mechanism	Nanoparticle	Mixing Time (min)	Sonication Time (min)	Solvent
Solvent Assisted Dispersion	Shear Forces, Cavitation-Implosion	MWCNT	NA	60	Acetone	[64]
	Shear Forces, Cavitation-Implosion	CNT	1440 (24h)		Ethanol	[65]
	Cavitation-Implosion	Alumina		30	Acetone	[66]
	Shear Forces	MWCNT		30	Acetone	[67]
	Shear Forces, Cavitation-Implosion	BNNP	30	10	Acetone	[68]

Note: MWCNT: multiwalled carbon nanotubes, CNT: Carbon nanotube, BNNP: Boron nitride nanoplatelets, MAM: poly (methyl methacrylate) blocks surrounding a center block of poly (butyl acrylate).

20 s on/off cycle) for 1 h [63]. Three roll-mill was instrumental in improving dispersion; where roller 1 and 3 rotate in anti-clockwise direction and roller 2 rotates in clockwise direction. Mill was operated at speed ratio of 1:3:9 with rpm of 180. Counter-rotation of successive rollers produces higher shear force. Additionally, varying gaps among the rollers and multiple passes of 20 mm (1st pass), 10 mm (2nd pass) and 5 mm (3rd pass) were used to generate high shear forces. Hardener was added to mixture and compound was stirred at 800 rpm for 10 min. A 30 min vacuum session was introduced prior to impregnate fiber through hand layup and curing through hot press. Fig. 3 exhibits the fabrication steps.

1.3.2. Solvent assisted dispersion

This method differs from direct mixing in usage of solvent to dilute epoxy and deagglomerate nanoparticles. Nor et al. followed an elaborate process to prepare glass/epoxy nanocomposites [64]. To deagglomerate MWCNT, required amount of MWCNT was dispersed initially in 150 mL acetone and stirred at 1000 rpm for 1 h. Bath sonication was done afterwards for an hour. High rotational motion in stirring and frequency waves in sonication generated shearing forces that helped induce deagglomeration. MWCNT/acetone mixture was introduced in epoxy. The epoxy/MWCNT/acetone mixture was then stirred at 70 °C and 1000 rpm to ensure acetone evaporation and simultaneous CNT dispersion. Epoxy/MWCNT mixture was sonicated at 70 °C for an additional 1 h. Entrapment of bubbles is obvious with sonication and shear mixing. Nanofluid, therefore, was kept under vacuum for 18 h prior to fabricating laminates using hand layup technique. Obradović et al. prepared Kevlar fiber reinforced poly vinyl butyral (PVB) composites decorated with CNT [65]. Desired weight of CNT was suspended in ethanol and sonicated for 30 min. This suspension was mixed with PVB-ethanol solution and stirred for 24 h. Impregnation of fiber was followed by hot press assisted curing at 170 °C, keeping pressure of 3 bar, for 15 min. Kaybal et al. prepared nanocomposites through solvent assisted dispersion of alumina nanoparticles in epoxy [66]. To deagglomerate nanoparticles, they were mixed with acetone. Solution was mixed to epoxy using ultrasonic energy for 30 min. Acetone was evaporated, afterwards, from epoxy using vacuum oven at 70 °C for 24 h.

Hardener was mixed with modified resin prior to two stage impregnations: Firstly, using hand layup and secondly, using VARTM. A schematic of the adopted process flow is provided in Fig. 4 (a) and homogeneous formulation in Fig. 4 (b).

Ismail et al. impressed by the importance of high shear forces, utilized mechanical stirring at 7500 rpm for 30 min to mix MWCNT dispersion in acetone [67]. After epoxy addition, solution was further stirred for 4 h. Hardener was introduced and mixture was agitated by hand. Modified resin was used, then, to impregnate fabric adopting hand layup. Ulus et al. dispersed boron nitride nanoplatelets in acetone for 10 min using sonicator [68]. Addition of BNNP suspension to epoxy was followed by two stage mixing: sonication for 10 min and mechanical stirring for 30 min. Compound was, then, heated at 70 °C for 24 h in a vacuum oven. Desired amount of hardener was introduced and manually mixed for 5 min. Owing to possible filtration of nanoparticles, impregnation was done using wet layup and curing using vacuum bagging. Table 1 presents summary of equipment and methods to introduce nanoparticles in matrices.

2. Discussion

Review of nanocomposite fabrication techniques helps highlight salient features and drawbacks of adopted methodologies. An obvious drawback of the direct mixing route is generation of bubbles during mechanical mixing of resin that necessarily require an additional step of bubble evacuation in vacuum oven. Higher viscosity of resin after nanoparticle addition leads to bubble entrapment. In solvent assisted dispersion, however, deagglomeration in acetone has been reported to effectively reduce net surface energy active during storage. Downside of this method is solvent evaporation step that prolongs the preparation time of nanocomposite. Another corollary of solvent addition is reactivity of solvent with resin that degrades the properties of resin especially in case of acetone. However, reduction in viscosity has been reported to improve dispersion of nanofillers [69].

A characteristic phenomenon that relates nanoparticle concentration to microstructure of nanocomposites can be glimpsed in Fig. 5. Fig. 5 (a) and (b) indicate acceptable van der Waals interaction among particles and

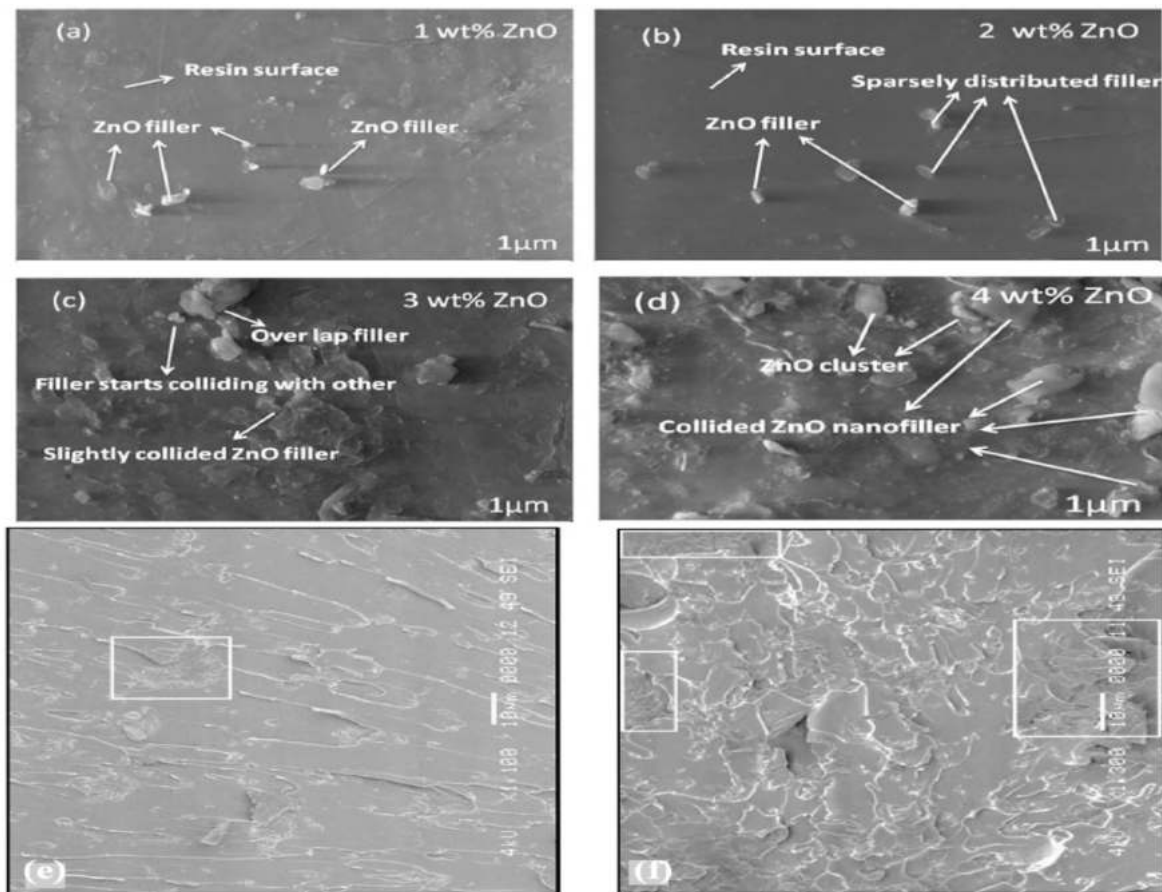


Fig. 5. Microstructure of ZnO reinforced epoxy at (a) 1 wt % (b) 2 wt % (c) 3 wt % and (d) 4 wt % [59], copyright 2019. Reproduced with authorization from Frontier Research Today. Increasing nanoclay clusters presence at (e) 1.5 and (f) 3 wt% of nanoparticle loading [61], copyright 2017. Reproduced with permission from Elsevier Ltd.

spheroid microstructure. Above 3 wt % concentration (Fig. 5 (c) and (d)), angular cluster formation starts that increases the agglomerate area in microstructure. Additionally, interparticle distance starts diminishing with non-homogeneous reinforcement of matrix. This study confirmed too that lower viscosity of resin, achieved through heating, was helpful in offering microstructural homogeneity; same rationale that makes solvent assisted dispersion promising.

In terms of mixing methods, often a combination of homogenizing techniques is effective such as shear mixing followed by sonication compared to a single technique like mechanical mixing. For instance, Rafiq et al. prepared clay nanocomposites with 1.5 and 3 wt % utilizing high shear mixer [61]. Fig. 5 (e) and (f) shows that clay clusters appeared with 1.5 and 3 wt% nanoclay concentration, respectively. In comparison, nanocomposite microstructure in Fig. 5 (a) and (b) validates that shear mixing followed by sonication helps breaks the agglomerates effectively and delays cluster formation to high nanoparticle loading level [59]. This stand out feature might stem from the fact that sonication energy dissipates effectively in localized vicinity thus effectively agitating the polymeric chains and nanoparticles to overcome van der Waals forces.

From Table 1, certain generalized conclusions can be derived despite the variety of equipment used by researchers and range of parameters adopted. Most of the studies employ combination of sonication and mechanical mixing to attain homogeneity. And reduction in resin viscosity is a common practice which in direct mixing and solvent assisted dispersion routes is achieved through resin heating and solvent addition, respectively. In general, if the nanoparticles are functionalized, a higher processing (mixing) time is considered necessary to allow interaction between functional groups and reactive epoxy sites [23].

2.1. Ballistic properties of nanocomposites

Ballistic impact in composites is a complex phenomenon that is influenced by material properties, target conditions and projectile parameters. Aside from these differences, a ballistic impact may end in one of the following three conditions.

- Projectile partially perforates the target indicating that the energy transferred to target is lower than the energy absorption capability of the target. A bounce back may happen in this case with projectile drop-off.
- Projectile perforates the target with zero residual velocity. This velocity is designated as ballistic limit pointing out to the fact that the total kinetic energy of projectile being absorbed by target.
- There is certain residual velocity after complete penetration of target. This indicates the higher value of initial kinetic energy than the energy target can absorb.

Last two conditions must prevail to estimate energy absorption of composite under ballistic loading. In the summary of nanocomposite properties presented, next, these conditions are believed to be fulfilled with following expression being used to calculate the absorbed energy.

$$V_{50} = \sqrt{V_s^2 - V_r^2}$$

$$E_{ab} = \frac{1}{2}mV_s^2 - mV_r^2$$

where m is the projectile mass in kg, V_s and V_r are the initial (striking)

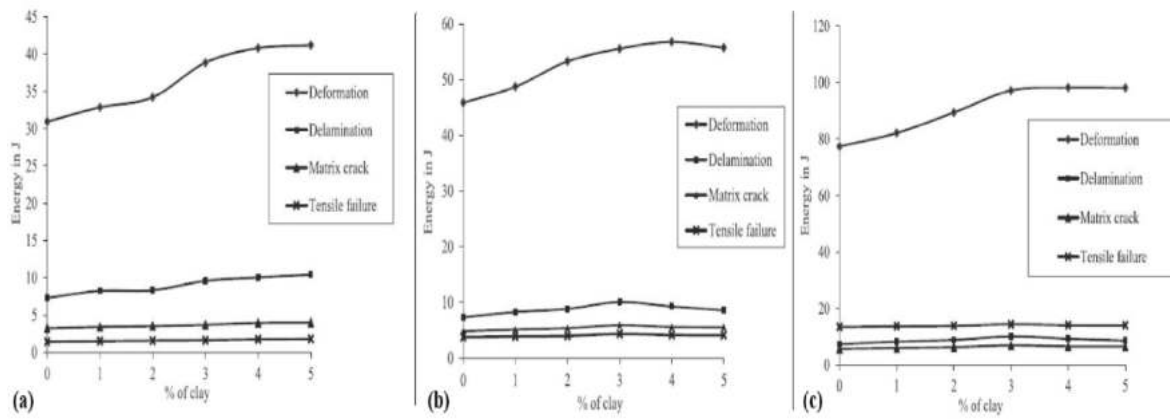


Fig. 6. Energy absorbed by laminates at (a) 130 m/s (3 layers) (b) 150 m/s (5 layers) and (c) 200 m/s (8 layers) [73], copyright 2014. Reproduced with permission from Elsevier Ltd.

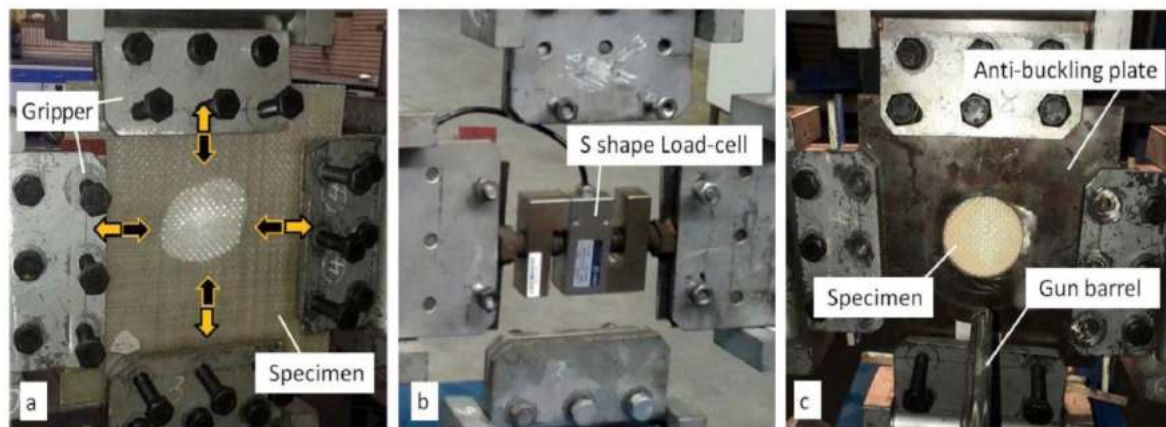


Fig. 7. (a) Bi-axial loading configuration (b) load cell assisted apparatus calibration and (c) anti-buckling plate assembly [78], copyright 2019. Reproduced with permission from Elsevier Ltd.

and residual velocity of the projectile, respectively [70].

2.1.1. Nanoclay

Nanoclays are essentially layered silicates with two structural elements: Si atom bound tetrahedrally and octahedrally shared Al(OH)₃/Mg(OH)₃ edge. Layered silicates are bound by weak van der Waals forces and retain high aspect ratio [71]. Optimum nanoparticle concentration has been of interest to researchers investigating ballistic attributes of composites. Pol et al. conducted experiments on plain weave E-glass/Epoxy composites incorporated with nanoclay, 0, 1, 2, 3, 5 and 7 wt %, at impact velocities of 130, 142 and 155 m/s [72]. Nanoclay were in platelets form and glass fiber fabric had an areal density of 200 g/m². Samples were prepared through vacuum assisted resin transfer molding with twelve layers of glass fabric and 60% fiber volume fraction. The results signified the importance of optimum nanoclay content in providing best impact properties. Among the three different velocities opted, maximum performance was of 99.97% energy absorption noted for 5% nano-clay composite at initial velocity of 130 m/s. Damage areas of 3336, 5832, 8631, 8799, 13,229 and 6031 mm² were noticed in increasing order of nanoclay content. Toughness of system (in 3–5 wt % range) increased along with decrease in fiber-matrix detachment. Also, presence of particles acted as crack arresters and decreased the density thereby increasing elastic, plastic and transverse wave velocities. This induced larger cone formation/damage area in 5% nano-clay sample.

Few studies focus on finding out effective order of energy absorption in various failure modes through experimental and modelling

approaches. For instance, Balaganesan used glass woven roving mats impregnated with nanoclay modified epoxy to prepare composites to be tested at various velocities [73]. Dispersion of clay varied from 1 to 5 wt %. In ballistic performance, presence of clay (4 wt %) improved energy absorption and prevented the stresses from reaching yield limit of fiber. (0⁰)₃ laminates with 0, 2, and 5 wt % nanoclay were perforated at 101.84, 122.32 and 129.51 m/s. For laminates tested above ballistic limit, residual velocities of nanocomposites were always lower than control samples. (0/45/0) laminate perforation velocities were 108.5 and 133 m/s at 0 and 5 wt % clay content, respectively. For (0⁰)₅ sequence, improvement in ballistic performance/limit were 5.4, 7.7, 9.2 and 10.8% for 2, 3, 4 and 5 wt % nanoclay, respectively. For (0/45/0/45/0) laminates with 2, 3, 4 and 5 wt % nanoclay, improvements noticed were 5.3, 6.8, 7.6 and 8.3%, respectively. The laminates with 2, 3, 4 and 5 wt% nanoclay, for (0⁰)₈ configuration, showed increase in ballistic limit of 5, 11.3, 15.6 and 17.5%, respectively. Fig. 6 depicts the trend of energy absorption, from highest to lowest, in various failure modes across three sample thicknesses and velocities. The trend is: deformation > delamination > matrix crack > tensile failure. Pol et al. incorporated organically modified MMT nanoclay in glass/epoxy composites at 0, 3, 5, 7 and 10 wt % loading ratio to investigate ballistic performance [77]. Plain woven glass fabric was used to prepare 2.6 mm thick laminate using hand layup. Target was impacted at 134 and 169 m/s with a flat-end steel projectile. An improvement in energy absorption of the order of 7.9 (at 134 m/s) and 18.9% (at 169 m/s) was noticed for 3 and 10 wt % samples compared to neat laminate. Theoretical

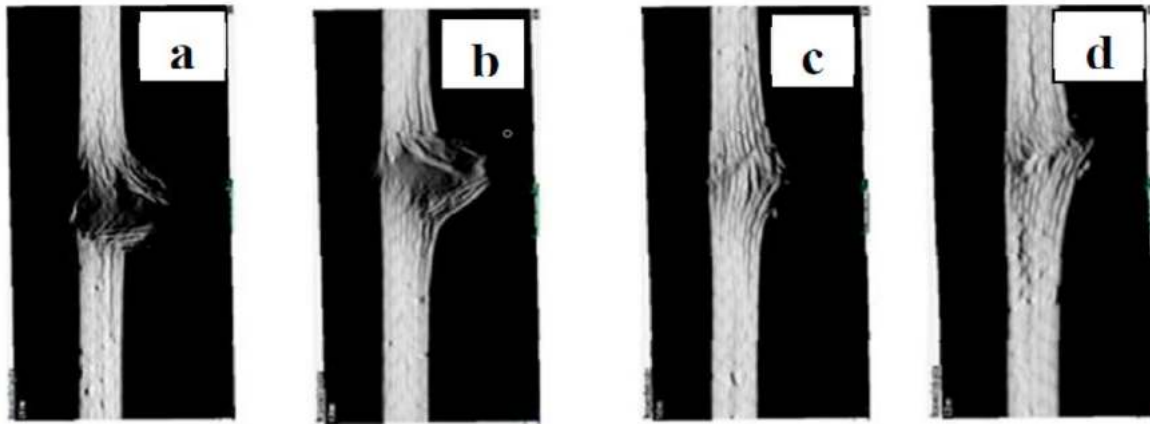


Fig. 8. CT scan images of side view of CFRP at (a) 0 (b) 1 (c) 3 and (d) 5 wt % of nanoclay [75], copyright 2018. Reproduced with permission from Elsevier Ltd.

model prediction highlighted following order of effective energy absorption mechanisms (from highest to lowest): cone kinetic energy, secondary yarn deformation, primary yarn failure and delamination for lower velocity; and cone kinetic energy, tensile failure of primary yarn, secondary yarn deformation and delamination for higher velocity. At 134 m/s, bottom layer damage areas were 12.2, 13.6, 11.8, 11.0 and 7.1 mm in ascending order of nanoclay content. At 169 m/s velocity, these values were 6.2, 7.5, 5.7, 6.0 and 7.7 mm in the same order. Damaged area of bottom layer reduced at high velocity indicating that contact duration is a key variable here. It was concluded that improvement in mechanical properties increased the perforation time (offered by contact resistance) which in turn improved the ballistic performance. Order of effective energy absorption mechanisms points out that higher contact duration enhances the role of secondary yarn deformation in total energy absorption contrary to higher importance of primary yarn tensile strength in lower contact duration scenario.

Few articles report altering variables like pre-loading conditions and laminate thickness to investigate nanocomposite performance. Moallemzadeh et al. investigated energy absorption and damage area relation of nanoclay modified glass/polyester composite with pre-loading conditions i.e. uniaxial tension, compression and biaxial tension/compression (Fig. 7(a)) [78]. Load cell were in-place to ensure proper calibration of equipment (Fig. 7 (b)). An optimum 1.5 wt % of nanoclay was used and ballistic tests were conducted in 138–185 m/s range. Cross-plyed laminate consisting of six layers were fabricated using hand layup. Steel-plates with aperture were utilized to apply pre-loads (1/3 of ultimate load) (Fig. 7 (c)). Generally, all nanocomposites fared better than non-modified composites in terms of energy absorption and residual velocity. Nanocomposite residual velocities were 19.9, 47, 19.3 and 36.7% lower than non-modified laminates for no-preloading, uniaxial tension, uniaxial compression and biaxial tension/compression loading arrangements, respectively. Worst performance of latter two conditions was attributed to micro-buckling and deterioration of interlaminar shear strength. Uniaxially pulled samples behaved better owing to greater alignment of fibers. Similarly, nanocomposites have higher damage area compared to neat composites in all conditions. At 185 m/s velocity, highest damage areas, in uniaxial tension, were 68 cm² and 25 cm² for modified and neat laminates, respectively. At 138 m/s impact velocity, damage areas for uniaxially compressed sample were 35 cm² (modified) and 27 cm² (neat) laminates, respectively. Anti-buckling plates were believed to restrict damage area extension used during compression loading.

Esfahani et al. varied nanoclay loading in glass/polyester composites to relate it with energy absorption in the range of 90–220 m/s impact velocity [79]. Laminates of 4, 8 and 12 layers with thickness in the range of 2.1–6.4 mm were prepared. Nanoclay loadings were 1.5 and 3 wt % by weight of resin. For analysis, velocities that did not induce complete

perforation were taken average to determine ballistic limit, V_{50} . Across different thicknesses, nanocomposites with 1.5 wt % nanoclay performed the best. V_{50} , for 4-, 8- and 12-layers laminates, were 19.79, 25.6 and 25.28% higher than respective neat samples. Energy absorption, at V_{50} , was 43.39, 59.55 and 56.89% superior to neat samples. Contact force was explained to be improved by nanocomposite compressive properties; and penetration and indentation kinetics were influenced by improved flexural properties. Also, V_{50} was shown to be linearly related to composite thickness regardless of nano-modification. Discussing failure modes, author concluded that back-face damage in thin-laminates (4 layers) was unaffected by nanoclay content. However, it increases (10–15 cm²) with increment in nanoclay content for mediumly thick (8 layers) laminates. Thick laminates (12 layers) were found to have optimum clay (1.5 wt %) content for maximum damage area (27 cm²). Dolati et al. did a preliminary study to investigate the best stacking sequence in terms of lowest damage area. E-glass fabric was impregnated with nanoclay modified epoxy [30]. Stacking sequences of [$\pm 45^0_3$]s and [$\pm 45^0/\pm 45^0$]s were chosen to prepare laminates consisting of six and four layers, respectively. Nanoclay at loading rates of 0.5, 1.5 and 3 wt%. were incorporated. Damage area reduced by 4.78 and 15.82%, at 0.5 and 1.5 wt % of nanoclay, for four-layer laminates. For six-layer laminate, 19.78% reduction in damage area was offered by 1.5 wt % laminate. Damage area increased at 3 wt % loading of nanoclay for both sample thicknesses owing to agglomeration and stress concentration. Additionally, fibre and matrix fracture were more extensive in four-layer sample.

In addition to glass/epoxy system, nanocomposites of carbon/epoxy have been tested for high velocity impact conditions. Pushparaja et al. investigated energy absorption of six-layers thick nanoclay modified carbon/epoxy laminate using ballistic test [74]. Nanoclay ratio was 0, 1, 3 and 5 wt %, and impact velocities were 110 and 125 m/s. Energy absorbed was calculated through initial and residual velocities difference. At 110 m/s velocity, 3 wt% nanoclay sample offered 75% improvement in absorbed energy compared to neat laminate. In general, above and below this nanoparticle concentration, energy absorption declined regardless of impact velocity. However, absorbed energy values for samples tested at 125 m/s were lower than those tested at 110 m/s. Absence of reflection peak in XRD pattern corroborated exfoliated structure of nanoclay, hence better energy transfer due to higher clay surface area in contact with epoxy. Delaminated area increased from 500 mm² (Neat) to 1750 mm² (3 wt %). Yarns experienced failure strains at point of impact and strain within elastic limit beyond impact point. Murugan et al. determined optimum nanoclay ratio for energy absorption of carbon/epoxy laminates under ballistic loading [75]. Samples containing 0, 1, 3 and 5 wt % of nanoclay were tested above ballistic limit velocities of 165, 195 and 220 m/s. Two thickness configurations of 3 and 6 mm were adopted for abovementioned nanoclay modification

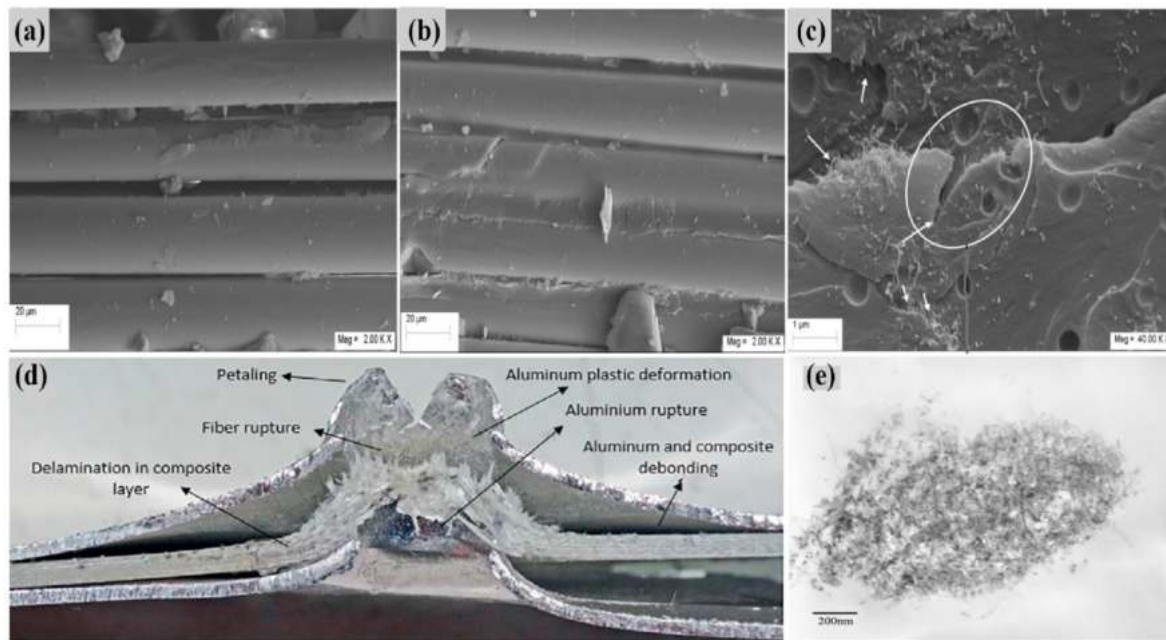


Fig. 9. Interfacial bonding in (a) 0 wt % (b) 0.3 wt % and (c) MWCNT bridging and pull-out in f-MWCNT nanocomposites. [63], copyright 2013. Reproduced with permission from Elsevier Ltd. (d) Damage modes in ballistic tested GLARE composites [86], copyright 2018, reproduced with permission from Elsevier Ltd. (e) CNT forests detected at higher nanoparticle loadings, copyright 2013. Reproduced with permission from Elsevier Ltd.

range. In 0–3 wt % range, performance improvement was indicated by lower residual velocity. Optimum nanoclay content was 3 wt % as it offered highest energy absorption for both thicknesses. Fractography, adopting X-ray CT scan, revealed front and back area being damaged, predominantly, owing to compression loading and tensile failure of yarns, respectively. Interestingly, damage area increased with nanoclay content which, author claimed to, have played role in improving penetration resistance of target. Scanning indicates, too, a higher plate bulge (cone radius) for neat (Fig. 8 (a)) and 1 wt % (Fig. 8 (b)) nanocomposite samples indicating reduced damage resistance. However, at optimum loading ratio (3 wt %), retardation of bulge formation (Fig. 8 (c)) showed improvement in fracture toughness.

Although most of the studies employ widely used laminate configurations, two studies applied principles of matrix modification to sandwich configurations of composites. Bahari-Sambran et al. used fiber metal laminate (Basalt Fiber-Epoxy/Aluminum) to investigate ballistic limit and energy absorption of composites by varying modified nanoclay percentage at 1, 3 and 5 wt % in epoxy [28]. Etchant was used to roughen metal surface; and tri-glycidoxy propyl trimethoxysilane introduced bond compatibility with epoxy. Four layers woven basalt fiber composite was sandwiched between aluminum sheets to be impacted at 118 m/s by conical aluminum projectile. An optimum 3 wt % of nanoclay improved ballistic limit velocity and energy absorption by 5% and 10%, respectively, compared to unmodified laminate. It was claimed that dentation and penetration phenomena were associated with compressive and flexural strength, respectively; both of which tested to be improved with nanoclay addition. Additionally, energy absorption improved due to higher shear strength among nanocomposite layers. Higher damage area for 3 wt % nanoclay sample was spotted with extensive fiber fracture in modified nanoclay samples owing to better fiber-matrix bond. Typical failures like core-face splitting and plastic deformation of metal was noticed too. No systematic attempt to calculate damage area was made. Nasirzadeh and sabet incorporates MMT nanoclay in polyurethane (PU) core at a loading ratio of 0, 0.25, 0.5, 1 and 3 wt % to investigate energy absorption and ballistic limit improvement of sandwich composites [76]. Face sheets consisted of three-layer glass/polyester composites prepared through wet layup.

Velocity range, adopted for testing, was 100–140 m/s. For 0.5 wt% sample, improvement of 15.5 and 27% in ballistic limit velocity and energy absorption were calculated. Both the energy absorption and ballistic limit velocity decreased in 1–3 wt % range of nanoclay. This was explained through stress concentration induced crack initiation at agglomerated nanoclay sites and brittle fracture of cells in modified foam (compressive modulus of cells increased 72% for 3 wt % sample). Additionally, as foam microstructure is cellular, higher nanoclay presence decreased cell diameter to wall thickness ratio. That means increment in brittle wall area altered fracture mode. Core-face splitting and propagation of radial cracks were dominant fracture modes, macroscopically.

2.1.2. Carbon nanotubes

A single-walled carbon nanotube is a graphene sheet bended at certain angles. The plane of bending consists of carbon atoms with sp^2 orbitals. CNT's differ depending upon the bending angle which in turn affect physical properties [80]. An appreciation of nanocomposite performance is evident when it is compared with neat composite efficiency at fixed nanoparticle loading. For example, Pandya et al. prepared flat panel of symmetric cross-ply laminates of glass fiber/epoxy dispersed with multiwalled carbon nanotube (MWCNT) [81]. CNT's were incorporated at a ratio of 0.5 wt % of resin. Fiber volume fraction was maintained at 0.63. A hardened steel ball of 7.6 g weight and 6.36 mm diameter was impacted on panels. Ballistic limit velocity for MWCNT dispersed laminate was noted to be 131 m/s, showing an increase of 3.1% compared to identical configuration prepared with neat resin. Damage extensions for neat and modified epoxy composites were 576.9 mm^2 and 369 mm^2 along bottom planes, an improvement of 36%. Micheli et al. investigated ballistic performance of eight ply Kevlar-Carbon fiber reinforced epoxy composites using firing railgun [83]. Railgun is an electromagnetic launcher that uses tunable power supplier to set capacitor charging voltage at required level. Bullet velocity can be adjusted as a function of energy of railgun. MWCNT, at 1 wt %, were utilized as epoxy modifier and two biaxial Kevlar layers were sandwiched between three carbon fiber layers. At 400 m/s, penetration did not occur as against 1000 m/s velocity where it occurred. A

qualitative comparison revealed higher hole surface area for nanofiller sample compared to virgin one at 1000 m/s. That indicated greater energy absorption induced by load transfer optimization. Additionally, stiffer matrix and MWCNT network induced immobility of fiber tows and damping, respectively. Tehrani et al. mixed 2 wt % of MWCNT in epoxy to prepare five-layer laminate consisting of plain weave carbon fabric. Impact energy absorption was investigated at a velocity of 500 m/s using hemispherical projectile. An improvement of 21% in energy absorption was noted compared to neat laminate. Increment in interlaminar fracture toughness, damping and buckling strength were considered responsible for better response. Quasi-static punch test revealed role of CNT-epoxy interphase failure and pull-out in enhancing energy absorption. Also, damage area width (1.3 cm) of both types of samples was equal. There was no explanation given how buckling strength of carbon fiber improved with CNT addition. On a global scale, its true owing to stiffness improvement due to CNT presence [87].

Functionalization of nanoparticles is believed to enhance epoxy-particle interaction thus offering niche to improve mechanical properties of composites. Naghizadeh et al. studied ballistic properties of carboxylic acid functionalized multi-walled carbon nanotubes (MWCNT) incorporated E-glass/Epoxy composites [82]. Both sonication and shear mixing were utilized to prepare 0.3, 0.5 and 1 wt % of COOH-MWCNT modified composites. Conical steel projectile ($m = 9.12$ g) was used to impact 8 layers thick panels, using gas-gun setup, at velocities of 85, 100 and 112 m/s. At 85 m/s, V_{bl} increment was 14.1%, 18.17% and 36.45% for 0.3, 0.5 and 1 wt % of COOH-MWCNT reinforced composites. Highest energy absorption of 86.19% was noted for 1 wt % of nanoparticle at 112 m/s. Relation between incident and residual velocities was linear as velocity range adopted was well above ballistic limit of material. Analysis of damaged pattern indicated retarded tendency of COOH-MWCNT composites to undergo severe damage. For example, 1 wt % CNT sample experienced bottom view damage of 1.21 cm² as against 4.46 cm² for neat composite. A general trend of enlarged fracture area was noticed with lower velocity possibly because higher contact time induced variety of energy absorption mechanisms such as matrix cracking and delamination. Rahman et al. incorporated amino-functionalized MWCNT's in glass/epoxy laminates to be tested in

velocity range of 240–380 m/s [63]. Nanotubes were mixed, at a ratio of 0.3 and 0.5 wt% of epoxy, through sonication and 3-roll shear mixer. Twelve-layer laminate was prepared using combination of hand layup and hot press; and tested using spherical projectile. Over the range of velocity adopted, 0.3 wt % sample turned out to be the best in energy absorbance with 7.7% improvement compared to neat laminate. Ultrasonic C-scan revealed lower projected damage area for nano-modified samples compared to neat laminates. A higher bending stiffness was believed to enhance energy absorption in terms of elastic deformation for modified laminates. Additionally, reduction in projected damage area for 0.3 (39.16 cm²) and 0.5 wt % (43.77 cm²) samples were 19.43 and 10.55%, respectively, with reference to control laminates (49.21 cm²). This phenomenon was corroborated through TEM micrographs wherein forests of CNT were found in 0.5 wt % composites as against homogeneous distribution of CNT's for 0.3 wt % nanocomposites. Additionally, improved fiber-matrix adhesion (Fig. 9 (a) and (b)), induced through proper mixing of nanoparticles, contribute to better stress transfers. Reactive sites of CNT and epoxy help generate an interlocked structure decorated with crack bridging (Fig. 9 (c)) to retard travel of cracks. It was believed that CNT forest pockets (Fig. 9 (e)) induced brittle failure thereby lowering energy absorption and compromising damage resistance, once crack travels through them.

Fiber surface-treatment is another promising way to control the mechanical properties of composites through enhanced surface area and roughness. Bodu et al. anchored CNT's on glass fabric using floating catalyst CVD method to investigate ballistic limit of 20-layer laminated composites. Two types of glass fabric were used: 21 μ m (GF1) diameter and 8 μ m (GF2) diameter [24]. GF2 fabric was treated with CNT and six GF2 layers interspersed in five-layer set of GF1 on top and bottom. Wet-layup fabrication was followed by compression molding. GF2 fabric underwent desizing before CNT anchoring and functionalization. Delamination was experienced by non-impact side interlaminar regions of neat laminates and middle interlaminar regions of modified composites. No attempt was made to calculate projected damage area. However, V_{50} value for modified laminate was 11.1% higher than that of neat laminate. Although purpose of using GF2 was to increase CNT forest density owing to higher surface area available, the delamination

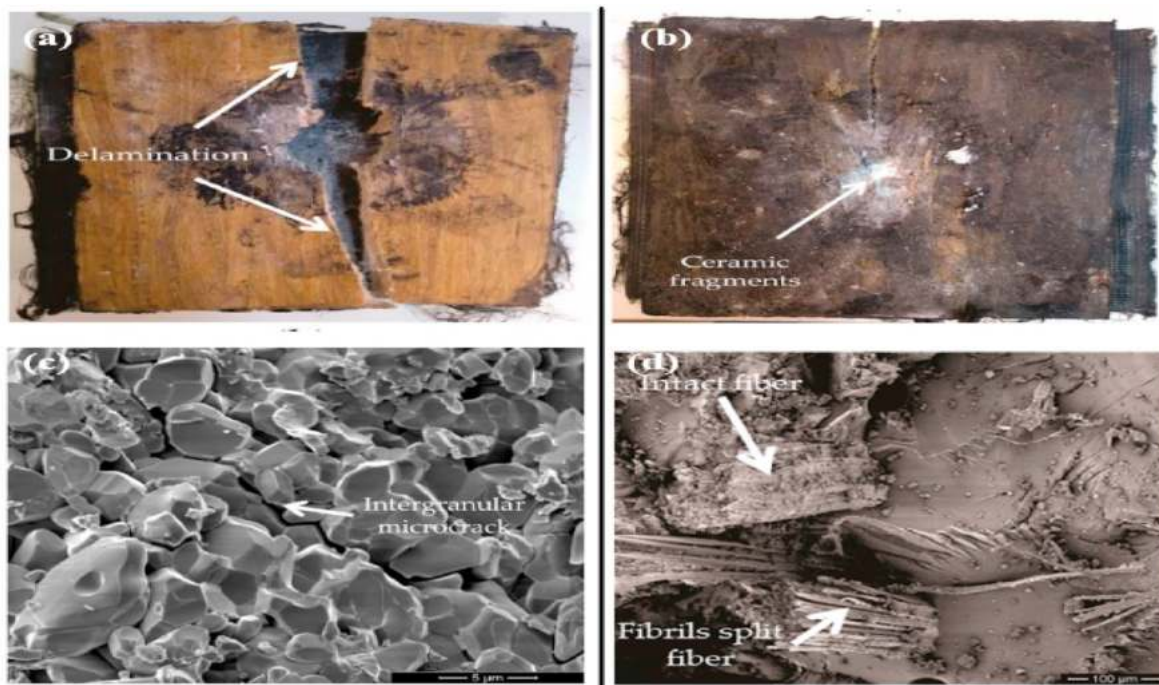


Fig. 10. Multilayer armor system upon (a) complete fracture of neat and (b) partial fracture of modified laminate (c) intergranular ceramic plate fracture (d) fibrillar failure of curaua fiber [88], copyright 2019. Reproduced with permission from MDPI.

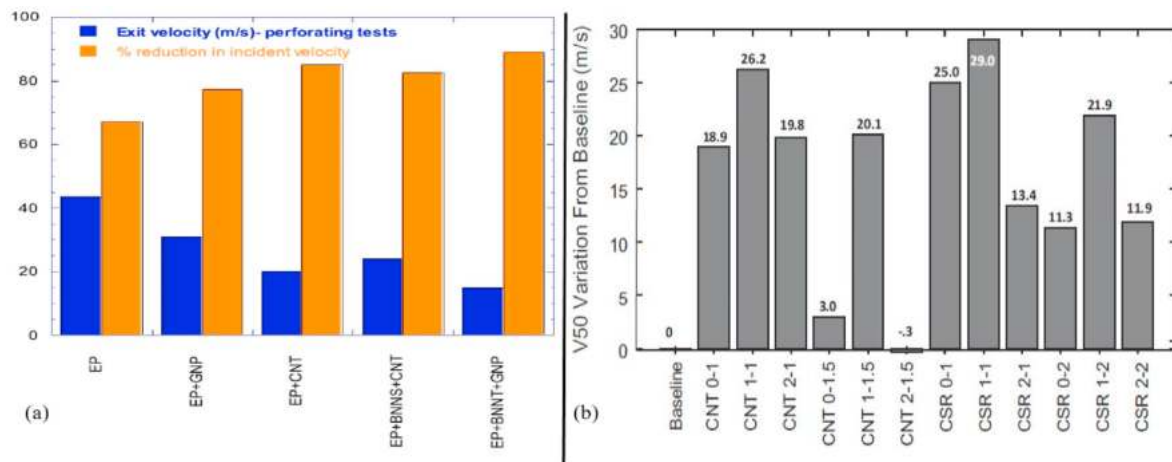


Fig. 11. (a) Percentage reduction in exit velocity of nanocomposites for perforating test [92], copyright 2019. Reproduced with permission from Elsevier Ltd. (b) Comparing increment in ballistic limit velocity of nanocomposites with baseline [91], copyright 2015. Reproduced with permission from Elsevier Ltd.

along treated fabric plane indicates weak/brittle interphase presence that is susceptible to radial wave energy induced damage.

Ballistic properties of nanocomposites employing sandwich configurations i.e. both core-face and FML have been tested too. Naghizadeh et al. investigated ballistic limit velocity and energy absorption of plywood core and E-glass/epoxy face-sheets sandwich structure under ballistic loading [84]. Carboxyl functionalized MWCNT modified epoxy and nylon matrices were used to prepare face-sheets. MWCNT concentration was identical in two face-sheets and varied in following range: 0, 0.3, 0.5 and 1 wt %. Nylon/glass face-sheet was adhesively bonded with core using epoxy. Ballistic limit velocities, obtained through fitting Lambert-Jonas equation with experimental data, improved by 4.78, 8.71, and 9.95% with 0.3, 0.5 and 1 wt % nanoparticle addition in epoxy. Similar trend continued for nylon composite with 5.5% improvement in V_{bl} for 1 wt % MWCNT. For a fixed projectile velocity, energy absorption increased with CNT concentration. V_{bl} was 11.24% higher for epoxy matrix laminate compared to nylon one. Damage area (98.48 cm²) for epoxy laminates was higher compared to nylon (3.5 cm²) laminates owing to longer perforation time induced by higher mechanical properties of epoxy face-sheets. However, damaged area decreased with increase in CNT concentration in both type of laminates. Khosravi and Farsani investigated energy absorption of CNT modified E-glass/epoxy anisogrid composite panels through ballistic testing [85]. Anisogrid panels consists of load bearing ribs diagonally attached to composite skin. CNT concentration varied from 0.1 to 0.5 wt % and initial velocity was 120 m/s. CNT's were surface modified through silane coupling agent to enhance interfacial interaction. An improvement in energy absorption was there, with 0.4 wt % nanocomposite offering 23% increment compared to neat sample. Retardation of interfacial frictional slippage, higher modulus and crack bridging were credited to have contributed to enhanced performance. At 0.5 wt %, property decline was attributed to CNT agglomeration. Similarly, damage area reduced up to 0.4 wt % nanoparticle loading and increased subsequently. Khoramishad et al. investigated energy absorption capacity of GLARE by incorporating MWCNT's at a loading ratio of 0.25, 0.5 and 1 wt % of epoxy matrix [86]. Stacking sequence was (Al/[Glass fiber/epoxy]₆/Al) and the laminate was impacted with spherical ball at 235 m/s. Highest energy absorption of 18.9% was attained at 0.5 wt % loading rate. After this loading ratio, energy absorption decreased. Damage mechanisms were identified in metal part (plastic deformation, petaling and rupture) and composite (fiber breakage, matrix cracking and delamination) parts (Fig. 5 (d)). In modified laminates, delamination and matrix cracking were suppressed owing to crack bridging and pull-out features. Additionally, greater deboning area of metal plates (37, 45, 53 and 48 mm for 0, 0.25, 0.5 and 1 wt % of CNT) was witnessed

for modified samples as against neat laminate presumably caused by decreased adhesion between metal and composite part. Also, improved fracture resistance of modified laminate was believed to cause deflection of crack to composite-metal interface thereby inducing higher debonding area.

2.1.3. Graphene nanoplatelets

This material is sometimes called super materials because of its exceptional mechanical properties. Graphene consists of sp² attached atom in hexagonal array. In a two-dimensional arrangement, carbon atoms maintain 0.142 nm distance between themselves. Each carbon atom is covalently bonded to three neighboring carbon atoms in lattice that imparts strength and rigidity to structure. Impact studies on graphene nanocomposites focus, predominantly, on investigating effect of thickness on performance. Priya and Vinyagam incorporated graphene nanoplatelets in epoxy to be used for woven glass fiber impregnation to investigate energy absorption under high velocity impact [89]. Two thicknesses i.e. 2 and 3 mm were prepared using four and six layers respectively through VARTM. Graphene concentration was maintained at 0.1 wt % of resin. For 2 mm thick sample, energy absorption was 9.5% higher than neat sample at an initial velocity of 150 m/s. Identically, energy absorption for 3 mm thick sample was 8.2% higher than neat sample at initial velocity of 145 m/s. Comparatively, performance of 3 mm sample is 12.8 (neat) and 11.8 (Modified) % higher than those of 2 mm counterparts. Author neither advanced rationale for thicker laminate performance nor presented damage area analysis. Naveen et al. prepared kevalr/cocosa nucifera-sheath reinforced modified (graphene nanoplatelets) epoxy hybrid composites to investigate energy absorption. Nanoparticles were dispersed in 0.25 and 0.5 wt % proportion to prepare nine- and twelve-layer laminates. A hemispherical projectile was shot in 300–320 m/s range using gas gun setup. At 0 wt % of GNP, nine-layer laminate offered lowest residual velocity across thicknesses. At 0.25 wt %, energy absorption increased, for instance, 8.5% compared to non-modified matrix. This trend existed for both 9- and 12-layer samples. Ballistic properties dropped at 0.5 wt % of GNP concentration owing to extra strong bonding. Author did not attempt to quantitatively discuss the damage area relation with nanoparticle loading.

Costa et al. applied graphene oxide coating on curaua fiber to reinforce epoxy matrix to be used as backing material in multilayered armor system [88]. Nanoparticles at loading ratio of 0.1 wt % of fiber were deposited. Shooting was conducted through 7.62 caliber ammunition on armor system with ceramic face and composite backing. Raman and FTIR analysis confirmed generation of new bonds on graphene-epoxy interface. None of the armor system experienced complete penetration of bullet. However, back face signature for graphene modified and

Table 2

Ballistic properties of Glass fiber/epoxy nanoparticle (BNNT/GNP/CNT/BNNS) composites [92], copyright 2019. Reproduced with permission from Elsevier Ltd.

Sample	Initial velocity (m/s)	Exit Velocity (m/s)	Decrease in Velocity (%)	Absorbed Energy (J)	SEA (kJ kg ⁻¹)
Neat Epoxy	131.6	43.6	67	218.9	1.77
EP + GNP	135	30.6	77.3	245.5	2.02
EP + CNT	135	20.1	85.1	253.9	1.92
EP + BNNS	135	23.9	82.3	250.7	2.06
EP + BNNT + GNP	135	14.7	89.1	255.7	1.91

non-modified composite were 27.4 and 25.6 mm. Contrastingly, non-modified sample broke apart (Fig. 10 (a)) whereas structural integrity of modified sample was there (Fig. 10 (b)). Ceramic plate was completely shattered with intergranular brittle fracture (Fig. 10 (c)) evident in microscope. Decline in performance was explained by higher modulus of coated fabric. A distinct aspect of energy absorption was fibrillar failure/debonding (Fig. 10 (d)) of curaua fiber due to absorption of shock waves. Author did not report bullet velocity that may indicate energy absorbed by the newly designed multilayered armor system.

2.1.4. Silica nanoparticles

Mesoporous structure and surface chemistry of silica nanoparticles have been of attraction to find out their potential application in nanocomposites [90]. For nanosilica studies, principle objective was to relate energy absorption and damage area with optimum nanoparticle concentration. Afrouzian et al. used modified epoxy to prepare twelve-layer glass/epoxy laminate to be tested under ballistic impact [70]. Silica nanoparticles at loading ratio of 0, 0.5, 1 and 3 wt % were utilized. Impact velocities lied in the range of 90–150 m/s to determine V_{50} . Generally, five specimens were tested for each concentration after estimating ballistic limit with first test. Highest ballistic limit, 110 m/s, was noticed for 0.5 wt% of nanocomposites. Similarly, highest absorbed energy of 56.3 J was associated with the same sample. At higher concentration of 3 wt %, both properties dropped indicating stress concentration owing to agglomeration. Investigation of damaged areas revealed highest value for virgin sample (10.5 cm²). For modified composites, values were 5.57, 6.5 and 8.2 cm² for 0.5, 1 and 3 wt % samples, respectively. Reduction in damage area points out that damage is getting localized with enhanced out-of-plane properties of composite, a phenomenon controlled by matrix. Nanoparticles presence retarded chain mobilization and activated toughening mechanisms in immediate area of impact. Naghizadeh et al. studied ballistic properties of silica incorporated E-glass/Epoxy composites [82]. Silica concentration was 0.5, 1, and 3 wt % of resin. Conical steel projectile of mass 9.12 g was used to impact 120 × 120 mm composite panels at velocities of 85, 100 and 112 m/s. By calculating ballistic limit velocity through taking square root of difference between initial and residual velocity, author determined increase in ballistic limit of the order of 11.45, 25.06 and 6.26% for 0.5, 1 and 3 wt % silica containing composites, at 85 m/s velocity. Highest improvement in energy absorption was 73.2% at 1 wt % of silica. For identical concentration, damage area reduced from 4.46 cm² to 1.39 cm².

Pandya et al. prepared flat panel of symmetric cross-ply laminates of glass fiber/epoxy dispersed with nanosilica at 1 wt % of resin [81]. A hardened steel ball of 7.6 g weight and 6.36 mm diameter was impacted on panels. By defining ballistic limit velocity, V_{50} , as the average of equal number of highest partial penetration velocities and lowest complete penetration velocities in a velocity range, V_{50} values of 127 m/s and 135 m/s were recorded for neat and modified configurations,

showing an increment of 6.3%. Damage area reduced for modified laminate (188.64 mm²) compared to neat laminate (576.9 mm²).

2.1.5. Composite nanoparticle

Nanoparticle suffer from fundamental problem of agglomeration owing to very high surface area. Primarily, addition of two or more types of nanoparticles, to prepare nanocomposites, aims at avoiding critical threshold concentration beyond which agglomeration is unavoidable in microstructure. Additionally, it provides niche to attain a set of properties emanating from distinct properties of each nanoparticle type. This technique has been adopted by few researchers to increase total nanoparticle concentration in composites. Manero II et al. prepared CNT and core-shell rubber particles to toughen Kevlar/epoxy composites [91]. Milled carbon fiber, CNT and rubber particles concentration varied from 0–2 wt % with milled fiber present in all samples. Mag 240 and 0.44 caliber bullets were used in a gun-powder barrel to determine V_{50} . 1st digit in the codes represent milled fiber concentration and 2nd digit shows CNT/rubber (CSR) concentration. It can be appreciated that all concentrations of nanoparticles and milled fiber increased V_{50} , except for 2 wt % milled carbon fiber and 1.5 wt % CNT combination (Fig. 11 (b)). An 8% improvement was vouchsafed by CSR 1-1. Consistent improvement in property with 1% milled fiber helped identify it as optimum loading level. Back-face deformation (2.87 cm) of modified and non-modified laminates was equal signifying energy absorption owing to matrix modification instead of kevlar fiber elongation. Domun et al. used multi walled boron nitride nanotubes (BNNT), functionalized boron nitride nanosheets (f-BNNS), functionalized multi walled carbon nanotubes (f-MWCNT) and graphene nanoplatelets (GNP) to prepare 24 layers composite panels with quasi-isotropic stacking sequence, (+45/90/-45/0)₃/(0/+45/90/-45)₃ [92]. Epoxy impregnation of fiber using hand layup was followed by vacuum assisted curing. Velocity of projectile was 134 m/s in penetrative impact test and 74 m/s in lower energy impact test. Performance improved for all modified epoxy samples compared to neat epoxy (Fig. 11 (a)). Highest reduction in exit velocity was 89.1% for epoxy modified with BNNT and GNP. Absorbed energy was 255.7 J for same sample, but with 8.7% more resin than neat epoxy sample. This fact can be discounted by adopting specific energy absorption (SEA) criteria which divides energy absorbed by mass of fiber (Table 2). Adopting this approach, epoxy modified with BNNS and CNT offered 16.3% higher SEA than neat epoxy. In low velocity impact scenario, minimum residual strain was associated with BNNT and GNP modified epoxy. In the same vein, damage in this laminate was highest which explains how impact energy was distributed in tensile failure of fibers, matrix crushing and interlaminar fracture with little to be remained for inducing residual strain.

Toorchi et al. studied nano-zirconia and graphene oxide loading ratio relation with impact energy absorption and V_{50} of the basalt/epoxy laminates [93]. Silane coupling agent was used to enhance bonding of nanomaterials with epoxy. Six-layer laminate were tested at 120 m/s velocity with a conical projectile. Nanoparticle loading varied for zirconia (0, 1, 2 and 3 wt %) and graphene oxide (0.1, 0.3 and 0.5 wt %). Graphene oxide nanocomposite offered improvement of 35 and 16% in energy absorption and ballistic limit velocity at 0.3 wt % loading. Similarly, 42 and 19% were the increment in energy absorption and limit velocity with 2 wt % of zirconia. highest improvements of 67 and 30% were for 0.1 wt % graphene oxide and 2 wt % zirconia reinforced sample. Reduced frictional slippage at interface, toughening of matrix and improved bending stiffness were attributed to be responsible for enhanced properties. In the same vein, damage area reduced by 53% (from 1215 to 570 mm²) compared to neat laminate for the last-mentioned configuration.

Gibson et al. determined ballistic properties of composite panels prepared with glass fiber/phenolic interleaved with carbon nanopaper and woven Kevlar/epoxy dispersed with MWCNT and milled fibers [94]. Ballistic limit standard was adopted, with delivery of projectile ensured through 44 mag soft point bullets and 30 caliber FSP (Fragment

Table 3

Compositions of the target laminates [97], copyright 2011. Reproduced with permission from Elsevier Ltd.

Target Identification	Sample Types	Thickness (mm)
1	Nanoclay 5 wt% + ceramic layer of nanoclay 25 wt%	10
2	Nanoclay 5 wt% + ceramic layer of nanoclay 33 wt%	10
3	No nanoclay (pure fiber glass/epoxy)	10
4	Nanoclay 5 wt% + pure fiber glass/epoxy	10
5	Graphene 3 wt% + pure fiber glass/epoxy	10

Table 4

Ballistic test results of 38 caliber special and 9 mm full metal jacket [97], copyright 2011. Reproduced with permission from Elsevier Ltd.

Projectile	Target	Energy (J)	BA (mm ²)	FA (mm ²)	BSC (mm)	Perforation
FMJ	1	576	3922	2652	–	Yes
	2	568	5158	2894	–	Yes
	3	582	2811	771	–	Yes
	3	446	5295	4431	13	No
	4	557	3103	550	16	No
SLP	4	442	2962	231	16.2	Yes
	5	445	3286	2395	17.0	Yes
	5	450	1389	231	8.2	No
	1	306	10,899	1341	5.0	No
	1	313	5588	501	7.5	No
	2	309	4994	6866	8.0	No
	3	280	1849	1176	–	Yes
	3	304	1032	231	7.9	No
	4	316	3762	4346	13	No
	5	302	3086	1030	14.0	No
5	284	1216	231	11.5	No	

simulated projectile). There was no significant improvement in ballistic limit of nanopaper interleaved composites and scant bonding was achieved among layers of glass fiber/phenolic laminates. MWCNT dispersed (at 0.5 wt %) composite with sixteen plies (44 mag) and thirty-two (30 caliber) plies laminates offered no improvement in ballistic limit when compared to neat resin counterparts. However, when 1.65 wt % of both milled fiber and MWCNT were incorporated in composites, an increment in performance of the order of 6.57% was obtained. Author concluded to stress influence of fracture toughness in offering higher V₅₀ value.

2.1.6. Other nanoparticles

In addition to the classification of nanocomposites described above, miscellaneous studies have been reported using not so famous

nanoparticles for impact property improvement of fiber reinforced composites. Fouda et al. determined reduction in velocity of projectile by incorporating iron oxide nanoparticles in carbon/epoxy laminates [95]. Concentrations of nanoparticles were 2.5 and 5 wt % of resin. Bullets of 9 mm and 7.5 mm were fired on 7- and 35-mm thick laminates, respectively. Reduction in residual velocity was 9% lower, for 5 wt % sample, when compared to neat laminate. The same value, for 7.5 mm armor piercing projectile and 35 mm thick sample, was 61% compared to neat laminate. Simić et al. prepared tungsten disulfide reinforced Kevlar/PVB + Phenolic laminates to determine back face deformation adopting NIJ standards [96]. Nanoparticles were dispersed at 3 wt % (fullerene-like) and 0.3 wt % (tube-like) of total mass of composite. Composites, consisted of twenty layers, were tested with 9 mm FMJ and 0.357 Magnum. A sixteen-layer sample, consisting of 1 wt % of fullerene-like and 0.2 wt % of tube-like nanoparticles, was prepared too. Cross-ply laminate did not stop any bullet and was outcasted. Plain weave laminate, with nanotube reinforcement, provided 13.8 and 14.3 mm back-face signature (lowest) for 9 mm and 0.357 Magnum projectile type, respectively, and completely stopped the bullet. Infrared camera recording identified sudden drop of temperature for neat laminate as against gradual drop for nano-reinforced laminate. This phenomenon was attributed to friction-generated heat active in nanocomposites.

Ávila et al. prepared fiber glass/epoxy/nanoclay and fiber glass/epoxy/nanographite samples. Velocities of 242 ± 6 m/s and 355 ± 23 m/s were arranged with 38 calibers special (SLP) and 9 mm full metal jacket (FMJ), respectively [97]. Amount of graphene nanosheets and nanoclay were 3 and 5 wt%. Fiber-matrix ratio was 65:35. Two types of ceramic layers were added to nanocomposites: first had three-part nanoclay and second had two-part nanoclay. Details of the samples are presented in Table 3.

Testing showed three distinct damage features: fiber breakage, intense delamination and diffused delamination. All nanocomposites exhibited less damaged area than control sample except target type 2 at front-face. In back signature criteria, all samples that did not undergo perforation had signature smaller than control sample. In case of energy absorption, 5 wt % configuration and control samples lied around lower bound energy of 306 J. Addition of ceramic layer increased the energy to around 316 J. Table 4 presents summary of ballistic test results. Intercalated presence of nanoparticle was responsible for higher impact energy. Also, their existence at fiber-matrix interface facilitated debonding due to their large surface area. It was concluded that nanoparticle addition changed the failure mode from intense crack propagation to interlaminar shear deformation due to their role as crack arrester.

Balaganeshan et al. utilized nanoclay to modify epoxy in loading range of 1–5 wt % of matrix [98]. Three layers glass/epoxy laminate were prepared to be tested in velocity range of 120–140 m/s with

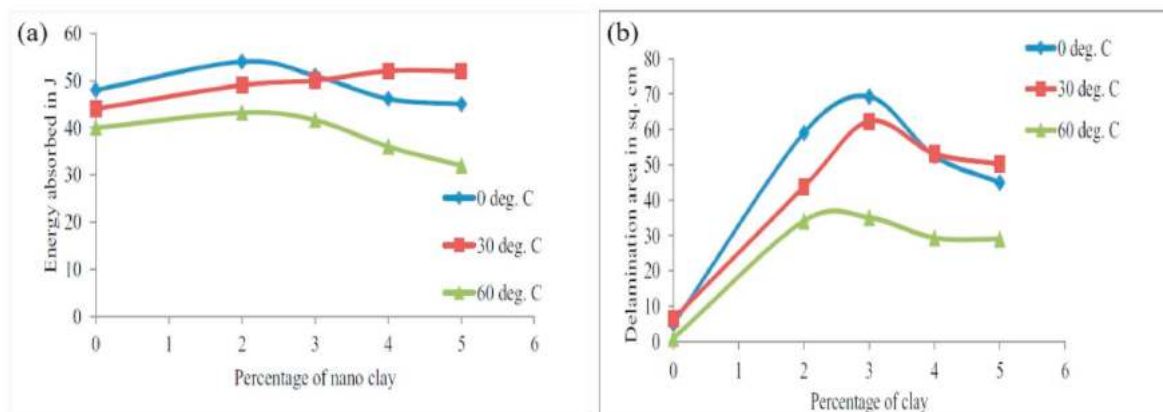


Fig. 12. (a) Energy absorption and (b) projected damage area profile with alteration in temperature for nanoclay reinforced laminates [98], copyright 2017. Reproduced with permission from Elsevier Ltd.

Table 5
Summary of ballistic performance and parameters/variables of nanocomposites.

Composite	Stacking Sequence	Reinforcement Type	Areal Weight (g/m ²)	No. of Layers	Projectile Geometry	Nanoparticle	Loading (wt. %)	Projectile Velocity Range (m/s)	Optimum Loading (wt. %)	Energy Absorption Improvement (%)	V ₅₀ (%)	Reference
Glass/Polyester (face) and PU (Core)		Plain weave	400	3	Conical	MMT nanoclay	0, 0.25, 0.5, 1 and 3	100–140	0.3	27	15.5	[76]
Glass/Epoxy		Plain weave	200		Flat End	MMT nanoclay	0, 3, 5, 7 and 10	134 and 169	3 and 10	7.9 and 18.95		[77]
Carbon/Epoxy		Woven	610	6	Conical	Nanoclay	0, 1, 3 and 5	110 and 125	3	75%		[74]
E-glass/Polyester	[0/90] ₆	Woven	400	6	Spherical	Nanoclay	1.5	138–185	1.5		30	[78]
E-glass/Polyester		Plain weave	400	4	Conical	Nanoclay	1.5 and 3	90–220	1.5	43.39	19.79	[79]
E-glass/Polyester		Plain weave	400	8	Conical	Nanoclay	1.5 and 3	90–220	1.5	59.55	25.6	[79]
E-glass/Polyester		Plain weave	400	12	Conical	Nanoclay	1.5 and 3	90–220	1.5	56.89	25.28	[79]
E-glass/Epoxy	[±45°] ₃ s	Woven	400	6	Conical	Nanoclay	0.5, 1.5 and 3	130–140	1.5	DA:19.78		[30]
E-glass/Epoxy	[±45°/±45°] _s	Woven	400	4	Conical	Nanoclay	0.5, 1.5 and 3	130–140	1.5	DA:15.8		[30]
Basalt Fiber-Epoxy/Aluminum	(Al/[Basalt-Epoxy] ₄ /Al)	Woven	NP	4	Conical	Nanoclay	1, 3 and 5	118	0.3	10	5	[28]
E-glass/Epoxy		Plain weave	200	12	Flat End	Nanoclay	0, 1, 2, 3, 5 and 7	130, 142 and 155	5%	99.97%		[72]
E-glass/Epoxy		Plain Weave	200	8	Conical	MWCNT	0.3, 0.5 and 1	85, 100 and 112	1	86.19		[82]
Glass/Epoxy	0/90	UD	500		Spherical	MWCNT	0.5	V ₅₀			3.1	[81]
Glass/Epoxy (face) and Plywood (Core)		Woven	200	8	Conical	MWCNT	0, 0.3, 0.5 and 1	NP	1		9.95	[84]
Glass/Nylon (face) and Plywood (Core)		Woven	200	8	Conical	MWCNT	0, 0.3, 0.5 and 1	NP	1		5.5	[84]
E-glass/Epoxy		Woven	258	12	Spherical	MWCNT	0.3 and 0.5	240–380	0.3	7.7	5–6	[63]
GLARE	(Al/[Glass fiber/epoxy] ₆ /Al)	Woven	200	6	Spherical	MWCNT	0.25, 0.5 and 1	235	0.5	18.9		[86]
Carbon/Epoxy		Woven	180	5	Spherical	MWCNT	2	500		21		[87]
E-glass/Epoxy		Anisogrid	258	4	Conical	CNT	0.1–0.5	120	0.4	23		[85]
E-glass/Epoxy		Plain weave	600	3	Conical	GNP	0.1	145–150	0.1	8.2		[89]
Basalt/Epoxy		Plain weave	300	6	Conical	Graphene oxide	0.1, 0.3 and 0.5	120	0.3	35	16	[93]
Kevlar/epoxy		Plain weave	474	NP	44 Mag/FSP	MWCNT + glass fiber	1.65 + 1.65	V ₅₀	NP		6.57	[94]
Glass/Epoxy	(+45/90/45/0) ₈	UD	NP	24	Conical	BNNT/GNP/CNT/BNNS	0.1 + 0.1	134 and 74	BNNS + CNT	16.3		[92]
Glass/Epoxy		Plain weave	200	12	Conical	Nanosilica	0, 0.5, 1 and 3	90–150	0.5	16.3	7.8	[70]
Basalt/Epoxy		Weave	300	6	Conical	Zirconia	1, 2 and 3	120	2	42	19	[93]

Note: DA: Delaminated area, UD: Unidirectional MWCNT: multiwalled carbon nanotubes, GNP: graphene nanoplatelets, CNT: Carbon nanotube, NP: Not provided, No. of layers are for fiber composite part.

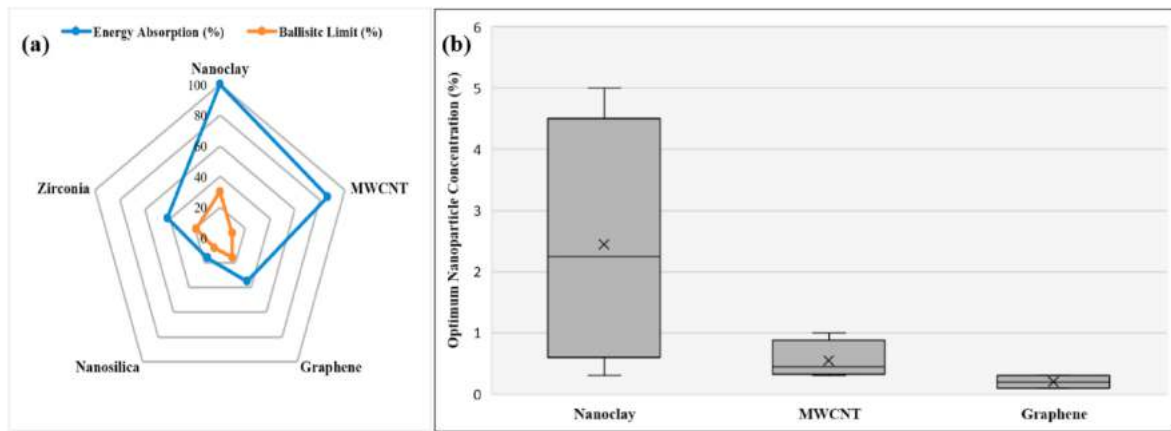


Fig. 13. (a) Maximum energy absorption and ballistic limit improvement reported for diverse nanocomposites (b) optimum nanoparticle concentration range of nanocomposites.

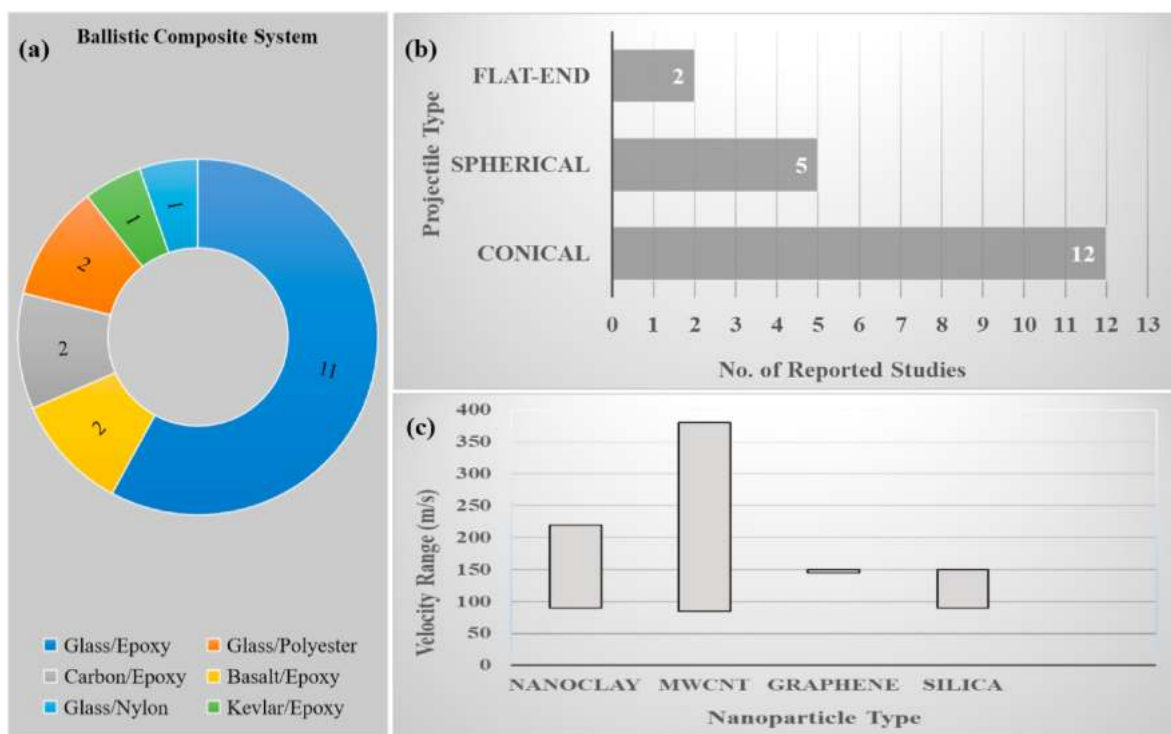


Fig. 14. (a) Various fiber reinforced nanocomposites (b) projectile types and (c) velocity range adopted for ballistic impact testing of glass fiber composites.

hemispherical projectile. A distinct aspect of the study was to determine energy absorption at temperatures of 0, 30 and 60 °C. Initial analytical results confirmed 31.5% higher energy absorption for clay-reinforced laminated in comparison with neat laminates. The energy absorption with variation in temperature profile is shown in Fig. 12 (a).

Among three temperature variations, highest value of energy absorption was for 5% clay sample at 30 °C. Optimum clay loading, at 0 °C and 60 °C, was 2 wt % whereas, at 30 °C, it was 5 wt %. At 30 °C, delaminated area (60 cm²) was 10 times higher, for 3 wt % loading, than the area of neat laminate (6.5 cm²) Fig. 12 (b). Two trends were obvious in delamination area studies: damage area increased for nanocomposites and damage at 0 °C is largest for laminates prepared with 0–4 wt % nanoparticle loading.

2.2. Analysis & discussion

Table 5 presents the summary of ballistic properties of nanocomposites prepared with variety of nanoparticles. There are property trends that can be identified when nanoparticles type is considered individually. For nanoclay reinforced composites, energy absorption and delamination resistance are the two parameters around which most of the studies are designed. In terms of energy absorption, highest percentage increase of 99.97% is reported; with general improvement lying in the range of 7.9–99.97% for various parameter and composite system tested. If we assume composite properties to be controlled by fiber properties, as tensile failure of primary yarns consumes highest amount of energy, these results are representative of glass fiber, as a fiber used most frequently, reinforced composites. Additionally, from the viewpoint of nanoparticle mechanical properties, nanoclay with strength and modulus values of 1 and 170 GPa [99,100], far less than CNT (10–60 and

300–1000 GPa) [101] and graphene (10–20 and 1000 GPa), potentially have contributed to enhanced toughness of composites by activating ductile fracture mechanisms [102,103]. It is known that rigid/stiff particles presence increases modulus of system [104]. Although other factors necessary for energy dissipation at high loading rates needs to be emphasized, concept of initiation of local shear yielding, at particle-matrix detachment, and void size should be understood [105]. That means, particle size should be smaller than critical polymer fracture size and it should have debonding strength lower than the yield strength of matrix.

For CNT reinforce composites, highest level of improvement was 86.19%. However, range of property improvement had been 7.7–86.19%. Here too, glass fiber was the choice of most researchers, presumably, owing to its higher strain to failure. For graphene nanocomposites, scarce studies defy a general conclusion, though improvement up to 35% was noticed for basalt-epoxy composites. The trend for maximum toughness improvement and ballistic limit, across nanoparticles tried, in microfiber composites has been shown in Fig. 13 (a).

A comparative glance at optimum concentration of different nanoparticles help identify the lower range for graphene and CNT compared to nanoclay. Critical concentration values are typically in the range of 0.3–5%, 0.3–1% and 0.1–0.3% for nanoclay, CNT and graphene, respectively (Fig. 13 (b)). That might hint at potential for improved performance for graphene nanocomposites at higher concentrations. Specific surface area might also explain this difference in threshold concentration [106]. Considering moderate specific surface area of MMT nanoclay ($265 \text{ m}^2/\text{g}$ [107]), its concentration range is much wider compared to MWCNT ($295\text{--}430 \text{ m}^2/\text{g}$ [108]) and graphene ($1019 \text{ m}^2/\text{g}$ [108,109]).

Additionally, certain generalized features of composite systems, especially glass fiber composites, tested for ballistic impact can be identified. E-glass is the choice of most researchers (Fig. 13 (a)) followed by basalt, carbon and kevlar fibers. Plain weave type reinforcement is predominantly used, in reviewed studies, primarily owing to superior piercing resistance of cross-weaved architecture [110]. A moderate areal weight of $200 \text{ g}/\text{m}^2$ was adopted in most of the studies in addition to 400 and $600 \text{ g}/\text{m}^2$. Epoxy and polyester were frequently utilized resins with nylon and phenolics present in the list too (Fig. 14 (a)). That signifies the importance of thermoset matrices in offering engineering properties together with their amenability to principles of matrix modification for mechanical property improvement. Among the different composites configurations, fiber reinforced thermoset matrices, fiber-metal laminates and sandwich structures, research activity, predominantly, revolves around impact property improvement of fiber reinforced thermoset matrix composites. Conical projectile was extensively utilized to test panels along with spherical balls and flat-end configuration (Fig. 14 (b)). As glass fiber was the only entity used for various nanoparticle composites, velocity range tested was easy to identify for glass fiber nanocomposite. Fig. 14 (c) provides the range of projectile velocity adopted for different nanocomposites.

3. Conclusion and perspective

Ballistic properties of composite materials are an interplay of matrix, reinforcement and interface performances. Major energy absorption mechanisms, therefore, are tensile failure of primary yarns, pull-up of secondary yarns, matrix and interface toughness. Diverse nano-scale toughness phenomena have been reported such as crack pinning, crack bridging and matrix chain immobilization to improve delamination resistance and energy absorption of laminated materials. Reviewed literature shows the importance of optimum nanoparticle content in both controlling damage area and energy absorption of the composite systems. Although, most of the researchers varied velocity in 50–500 m/s range, an obvious conclusion was that of improved performance, in terms of energy absorption and damage resistance, of nanocomposites compared to neat laminates within this range. Nanoclay and CNT's, as

frequently utilized nanoparticles, showed toughness improvement range of 7.9–99.97% and 7.7–86.19%, respectively. There are few avenues of ballistic research that needs to be explored to shed further light on polymer nanocomposite properties.

- 1 Composite structures experience variety of in-service temperature conditions. Testing fiber reinforced nanocomposite under specific conditions such as cryo-temperatures will help draw performance comparison with neat composites when tested in high velocity regimes.
- 2 Adopting surface modification principles, simultaneous modification of both microfiber and nanoparticles may open a possibility to control performance through interfaces.
- 3 Interlaminar region has been successfully designed through CNT growth on fibers, nanoparticle alignment and nanoparticle mats to improve Mode I and II properties. It will be worthwhile to investigate efficiency of these designs against damage resistance and for energy absorption in ballistic regime.
- 4 Mechanics of fiber reinforced nanocomposites in ballistic regime is an overlooked area that has potential to open new vistas in nanocomposite designs and understanding of nano and micro-scale factors contributing to macro-scale performance.
- 5 Polymer nanocomposites are reported to both increase and decrease damage areas upon impact. This apparent anomaly might stem from variety of adopted damage detection techniques and damage areas studied as evident in terms: bottom area delamination and projected damage area. There is a need to formulate standardized practices suitable for detection of damage in different regions of laminates to arrive at proper conclusions regarding relation of matrix modifications with damage types.

With current interest in nanoparticles assisted tailoring of properties, composites materials may promise advanced performance required in aircraft and automotive structures under complex ballistic impact conditions.

Declaration of competing interest

The authors declare that they have no known competing financial interests or personal relationships that could have appeared to influence the work reported in this paper.

Acknowledgement

First author would like to thank Higher Education Commission, Pakistan for providing financial assistance. This work was accomplished with monetary assistance provided by Universiti Teknologi Malaysia through grant number Q. J130000.2409.07G99. Additionally, authors acknowledge courtesy of Center for Advanced Research in Fluid Flow (CARIFF), UMP for allowing their facilities to be used for research.

References

- [1] A.B. Strong, *Fundamentals of Composites Manufacturing: Materials, Methods and Applications*, Society of Manufacturing Engineers 2008.
- [2] P. Mangalgiri, *Composite materials for aerospace applications*, *Bull. Mater. Sci.* 22 (3) (1999) 657–664.
- [3] E.P. Fahrenthold, R.J. Hernandez, *Simulation of orbital debris impact on the space shuttle wing leading edge*, *IJIE* 33 (1–12) (2006) 231–243.
- [4] W.P. Schonberg, *Hole size and crack length models for spacecraft walls under oblique hypervelocity projectile impact*, *Aero. Sci. Technol.* 3 (7) (1999) 461–471.
- [5] E.E. Herricks, D. Mayer, S. Majumdar, *Foreign Object Debris Characterization at a Large International Airport*, 2015.
- [6] R. Olsson, *Low-and Medium-Velocity Impact as a Cause of Failure in Polymer Matrix Composites*, *Failure Mechanisms in Polymer Matrix Composites*, Elsevier, 2012, pp. 53–78.
- [7] B.Y. Kolesnikov, L. Herbeck, *Carbon Fiber Composite Airplane Fuselage: Concept and Analysis*, IIA international conference, Berlin, 2004.

- [8] C. Ulven, U. Vaidya, M. Hosur, Effect of projectile shape during ballistic perforation of VARTM carbon/epoxy composite panels, *CmpSt* 61 (1–2) (2003) 143–150.
- [9] T. Mitrevski, I.H. Marshall, R. Thomson, R. Jones, B. Whittingham, The effect of impactor shape on the impact response of composite laminates, *CmpSt* 67 (2) (2005) 139–148.
- [10] G. Cicala, S. Mannino, G. Cozzo, A. Latteri, Novel polymeric systems for high performance liquid molding technologies, *Recent Research Developments in Polymer Science* 11 (2012) 77–97.
- [11] N. Chikhi, S. Fellahi, M. Bakar, Modification of epoxy resin using reactive liquid (ATBN) rubber, *Eur. Polym. J.* 38 (2) (2002) 251–264.
- [12] M. Groleau, Y.-B. Shi, A. Yee, J. Bertram, H. Sue, P. Yang, Mode II fracture of composites interlayered with nylon particles, *Compos. Sci. Technol.* 56 (11) (1996) 1223–1240.
- [13] M. Hojo, S. Matsuda, M. Tanaka, S. Ochiai, A. Murakami, Mode I delamination fatigue properties of interlayer-toughened CF/epoxy laminates, *Compos. Sci. Technol.* 66 (5) (2006) 665–675.
- [14] C. Atas, O. Sayman, An overall view on impact response of woven fabric composite plates, *CmpSt* 82 (3) (2008) 336–345.
- [15] B. Schrauwen, T. Peijs, Influence of matrix ductility and fibre architecture on the repeated impact response of glass-fibre-reinforced laminated composites, *ApCM* 9 (6) (2002) 331–352.
- [16] B. Vieille, V.M. Casado, C. Bouvet, Influence of matrix toughness and ductility on the compression-after-impact behavior of woven-ply thermoplastic-and thermosetting-composites: a comparative study, *CmpSt* 110 (2014) 207–218.
- [17] T. Yokozeki, A. Kuroda, A. Yoshimura, T. Ogasawara, T. Aoki, Damage characterization in thin-ply composite laminates under out-of-plane transverse loadings, *CmpSt* 93 (1) (2010) 49–57.
- [18] H. Hajiha, M. Sain, High toughness hybrid biocomposite process optimization, *Compos. Sci. Technol.* 111 (2015) 44–49.
- [19] R. Yahaya, S. Sapuan, M. Jawaid, Z. Leman, E. Zainudin, Quasi-static penetration and ballistic properties of kenaf–aramid hybrid composites, *Mater. Des.* 63 (2014) 775–782.
- [20] R. Petrucci, C. Santulli, D. Puglia, E. Nisini, F. Sarasini, J. Tirillò, L. Torre, G. Minak, J. Kenny, Impact and post-impact damage characterisation of hybrid composite laminates based on basalt fibres in combination with flax, hemp and glass fibres manufactured by vacuum infusion, *Composites Part B* 69 (2015) 507–515.
- [21] F. Sarasini, J. Tirillò, S. D’Altilia, T. Valente, C. Santulli, F. Touchard, L. Chocinski-Arnault, D. Mellier, L. Lampani, P. Gaudenzi, Damage tolerance of carbon/flax hybrid composites subjected to low velocity impact, *Composites Part B* 91 (2016) 144–153.
- [22] A.K. Bandaru, S. Patel, Y. Sachan, R. Alagirusamy, N. Bhatnagar, S. Ahmad, Low velocity impact response of 3D angle-interlock Kevlar/basalt reinforced polypropylene composites, *Mater. Des.* 105 (2016) 323–332.
- [23] E.M. Soliman, M.P. Sheyha, M.R. Taha, Low-velocity impact of thin woven carbon fabric composites incorporating multi-walled carbon nanotubes, *IJIE* 47 (2012) 39–47.
- [24] V.M. Boddu, M.W. Brenner, J.S. Patel, A. Kumar, P.R. Mantena, T. Tadepalli, B. Pramanik, Energy dissipation and high-strain rate dynamic response of E-glass fiber composites with anchored carbon nanotubes, *Composites Part B* 88 (2016) 44–54.
- [25] M. Siochi, *Structural Nanocomposites for Aerospace Applications*, 2015.
- [26] S. Trimble, Lockheed Martin reveals F-35 to feature nanocomposite structures. <https://www.flightglobal.com/lockheed-martin-reveals-f-35-to-feature-nanocomposite-structures/100174.article>, 2011.
- [27] J. Liu, H. Liu, C. Kaboglu, X. Kong, Y. Ding, H. Chai, B.R. Blackman, A.J. Kinloch, J.P. Dear, The impact performance of woven-fabric thermoplastic and thermoset composites subjected to high-velocity soft-and hard-impact loading, *ApCM* 26 (5) (2019) 1389–1410.
- [28] F. Bahari-Sambran, R. Eslami-Farsani, S. Arbab Chirani, The flexural and impact behavior of the laminated aluminum-epoxy/basalt fibers composites containing nanoclay: an experimental investigation, *J. Sandw. Struct. Mater.* (2018), 1099636218792693.
- [29] G. Dresselhaus, M. Pimenta, R. Saito, J. Charlier, S. Brown, P. Corio, A. Marucci, M. Dresselhaus, D. Tománek, R. Enbody, Science and applications of nanotubes, *Proceedings of Nanotube* 99 (2000) 24–27.
- [30] S. Dolati, A. Fereidoon, A. Sabet, Hail impact damage behaviors of glass fiber reinforced epoxy filled with nanoclay, *JCoMa* 48 (10) (2014) 1241–1249.
- [31] N. Nash, T. Young, P. McGrail, W. Stanley, Inclusion of a thermoplastic phase to improve impact and post-impact performances of carbon fibre reinforced thermosetting composites—a review, *Mater. Des.* 85 (2015) 582–597.
- [32] N. Razali, M. Sultan, F. Mustapha, N. Yidris, M. Ishak, Impact damage on composite structures—a review, *Int. J. Eng. Sci.* 3 (7) (2014), 08–20.
- [33] M. Ali, S. Joshi, M.T.H. Sultan, Palliatives for low velocity impact damage in composite laminates, *Advances in Materials Science and Engineering* (2017) 2017.
- [34] J.J. Andrew, S.M. Srinivasan, A. Arokiaarajan, H.N. Dhakal, Parameters influencing the impact response of fiber-reinforced polymer matrix composite materials: a critical review, *CmpSt* (2019) 111007.
- [35] S. Clifton, B. Thimmappa, R. Selvam, B. Shivamurthy, Polymer nanocomposites for high-velocity impact applications—A review, *Composites Communications* 17 (2020) 72–86.
- [36] A.P. Kumar, D. Depan, N.S. Tomer, R.P. Singh, Nanoscale particles for polymer degradation and stabilization—trends and future perspectives, *Prog. Polym. Sci.* 34 (6) (2009) 479–515.
- [37] H. Zhang, Z. Zhang, K. Friedrich, C. Eger, Property improvements of in situ epoxy nanocomposites with reduced interparticle distance at high nanosilica content, *Acta Mater.* 54 (7) (2006) 1833–1842.
- [38] B. Johnsen, A. Kinloch, R. Mohammed, A. Taylor, S. Sprenger, Toughening mechanisms of nanoparticle-modified epoxy polymers, *Polymer* 48 (2) (2007) 530–541.
- [39] F.H. Gojny, M.H. Wichmann, B. Fiedler, K. Schulte, Influence of different carbon nanotubes on the mechanical properties of epoxy matrix composites—a comparative study, *Compos. Sci. Technol.* 65 (15–16) (2005) 2300–2313.
- [40] M.H. Wichmann, K. Schulte, H.D. Wagner, On nanocomposite toughness, *Compos. Sci. Technol.* 68 (1) (2008) 329–331.
- [41] A. Kelly, Interface effects and the work of fracture of a fibrous composite, *Proceedings of the Royal Society of London. A. Mathematical and Physical Sciences* 319 (1536) (1970) 95–116.
- [42] M. Inagaki, F. Kang, Engineering and Applications of Carbon Materials, Butterworth-Heinemann, Waltham, MA, 2014, pp. 219–525.
- [43] A. Asadi, K. Kalaitzidou, Process-Structure-Property Relationship in Polymer Nanocomposites, Experimental Characterization, Predictive Mechanical and Thermal Modeling of Nanostructures and Their Polymer Composites, Elsevier, 2018, pp. 25–100.
- [44] I. Khan, K. Saeed, I. Khan, Nanoparticles: properties, applications and toxicities, *Arabian Journal of Chemistry* 12 (7) (2019) 908–931.
- [45] S. Billah, Composites and Nanocomposites, 2019, pp. 447–512.
- [46] Y.-Q. Li, S.-Y. Fu, Y.-W. Mai, Preparation and characterization of transparent ZnO/epoxy nanocomposites with high-UV shielding efficiency, *Poly* 47 (6) (2006) 2127–2132.
- [47] J.N. Coleman, M. Lotya, A. O’Neill, S.D. Bergin, P.J. King, U. Khan, K. Young, A. Gaucher, S. De, R.J. Smith, Two-dimensional nanosheets produced by liquid exfoliation of layered materials, *Science* 331 (6017) (2011) 568–571.
- [48] Y. Ou, F. Yang, Z.Z. Yu, A new conception on the toughness of nylon 6/silica nanocomposite prepared via in situ polymerization, *J. Polym. Sci., Part B: Polym. Phys.* 36 (5) (1998) 789–795.
- [49] J. Sandler, J. Kirk, I. Kinloch, M. Shaffer, A. Windle, Ultra-low electrical percolation threshold in carbon-nanotube-epoxy composites, *Poly* 44 (19) (2003) 5893–5899.
- [50] P. Rawat, K.K. Singh, Damage tolerance of carbon fiber woven composite doped with MWCNTs under low-velocity impact, *Proc. eng.* 173 (2017) 440–446.
- [51] A. El Moumen, M. Tarfaoui, K. Lafdi, H. Benyahia, Dynamic properties of carbon nanotubes reinforced carbon fibers/epoxy textile composites under low velocity impact, *Composites Part B* 125 (2017) 1–8.
- [52] R. Amooiy Dizaji, M. Yazdani, E. Aligholizadeh, A. Rashed, Effect of 3D-woven glass fabric and nanoparticles incorporation on impact energy absorption of GLARE composites, *Polym. Compos.* 39 (10) (2018) 3528–3536.
- [53] S. Denneulin, P. Viot, F. Leonard, J.-L. Lataillade, The influence of acrylate triblock copolymer embedded in matrix on composite structures’ responses to low-velocity impacts, *CmpSt* 94 (4) (2012) 1471–1481.
- [54] K.R. Ramakrishnan, S. Guerdar, P. Viot, K. Shankar, Effect of block copolymer nano-reinforcements on the low velocity impact response of sandwich structures, *CmpSt* 110 (2014) 174–182.
- [55] E.G. Koricho, A. Khomenko, M. Haq, L.T. Drzal, G. Belingardi, B. Martorana, Effect of hybrid (micro-and nano-) fillers on impact response of GFRP composite, *CmpSt* 134 (2015) 789–798.
- [56] M.K. Hossain, M.M.R. Chowdhury, K.A. Imran, M.B. Salam, A. Tauhid, M. Hosur, S. Jeelani, Effect of low velocity impact responses on durability of conventional and nanophased CFRP composites exposed to seawater, *Polym. Degrad. Stabil.* 99 (2014) 180–189.
- [57] A.S. Rahman, V. Mathur, R. Asmatulu, Effect of nanoclay and graphene inclusions on the low-velocity impact resistance of Kevlar-epoxy laminated composites, *CmpSt* 187 (2018) 481–488.
- [58] J. Qiu, C. Zhang, B. Wang, R. Liang, Carbon nanotube integrated multifunctional multiscale composites, *Nano* 18 (27) (2007) 275708.
- [59] K.D. Kumar, Synthesis and prediction of surface morphology, physical and mechanical properties of functionalized nano zinc-oxide embedded in unidirectional S-glass fiber epoxy composites, *Frontier Research Today* 2 (2019) 2006.
- [60] M. Landowski, G. Strugała, M. Budzik, K. Imielińska, Impact damage in SiO₂ nanoparticle enhanced epoxy–Carbon fibre composites, *Composites Part B* 113 (2017) 91–99.
- [61] A. Rafiq, N. Merah, R. Boukhili, M. Al-Qadhi, Impact resistance of hybrid glass fiber reinforced epoxy/nanoclay composite, *Polym. Test.* 57 (2017) 1–11.
- [62] T.H. Mahdi, M.E. Islam, M.V. Hosur, S. Jeelani, Low-velocity impact performance of carbon fiber-reinforced plastics modified with carbon nanotube, nanoclay and hybrid nanoparticles, *J. Reinforc. Plast. Compos.* 36 (9) (2017) 696–713.
- [63] M. Rahman, M. Hosur, S. Zainuddin, U. Vaidya, A. Tauhid, A. Kumar, J. Trovillion, S. Jeelani, Effects of amino-functionalized MWCNTs on ballistic impact performance of E-glass/epoxy composites using a spherical projectile, *IJIE* 57 (2013) 108–118.
- [64] A.F.M. Nor, M.T.H. Sultan, M. Jawaid, A.M.R. Azmi, A.U.M. Shah, Analysing impact properties of CNT filled bamboo/glass hybrid nanocomposites through drop-weight impact testing, UWPI and compression-after-impact behaviour, *Composites Part B* 168 (2019) 166–174.
- [65] V. Obradović, D. Stojanović, I. Živković, V. Radojević, P. Uskoković, R. Aleksić, Dynamic mechanical and impact properties of composites reinforced with carbon nanotubes, *Fibers Polym.* 16 (1) (2015) 138–145.
- [66] H.B. Kaybal, H. Ulus, O. Demir, Ö.S. Şahin, A. Avci, Effects of alumina nanoparticles on dynamic impact responses of carbon fiber reinforced epoxy

- matrix nanocomposites, *Engineering Science and Technology, an International Journal* 21 (3) (2018) 399–407.
- [67] K. Ismail, M. Sultan, A. Shah, M. Jawaid, S. Safri, Low velocity impact and compression after impact properties of hybrid bio-composites modified with multi-walled carbon nanotubes, *Composites Part B* 163 (2019) 455–463.
- [68] H. Ulus, T. Üstün, Ö.S. Şahin, S.E. Karabulut, V. Eskizeybek, A. Avcı, Low-velocity impact behavior of carbon fiber/epoxy multiscale hybrid nanocomposites reinforced with multiwalled carbon nanotubes and boron nitride nanoplates, *JCoMa* 50 (6) (2016) 761–770.
- [69] M.R. Loos, L.A.F. Coelho, S.H. Pezzin, S.C. Amico, The effect of acetone addition on the properties of epoxy, *Polímeros* 18 (1) (2008) 76–80.
- [70] A. Afrouzian, H. Movahhedi Aleni, G. Liaghat, H. Ahmadi, Effect of nano-particles on the tensile, flexural and perforation properties of the glass/epoxy composites, *J. Reinforc. Plast. Compos.* 36 (12) (2017) 900–916.
- [71] K.G. Bhattacharyya, S.S. Gupta, Adsorption of a few heavy metals on natural and modified kaolinite and montmorillonite: a review, *Adv. Colloid Interface Sci.* 140 (2) (2008) 114–131.
- [72] M.H. Pol, G. Liaghat, F. Hajiarazi, Effect of nanoclay on ballistic behavior of woven fabric composites: experimental investigation, *J. Compos. Mater.* 47 (13) (2013) 1563–1573.
- [73] R. Velmurugan, G. Balaganesan, Energy absorption characteristics of glass/epoxy nano composite laminates by impact loading, *Int. J. Crashworthiness* 18 (1) (2013) 82–92.
- [74] M. Pushparaja, G. Balaganesan, R. Velmurugan, N. Gupta, Energy absorption characteristics of carbon/epoxy nano filler dispersed composites subjected to localized impact loading, *Procedia engineering* 173 (2017) 175–181.
- [75] P. Murugan, K. Naresh, K. Shankar, R. Velmurugan, G. Balaganesan, High velocity impact damage investigation of carbon/epoxy/clay nanocomposites using 3D Computed Tomography, *Mater. Today: Proceedings* 5 (9) (2018) 16946–16955.
- [76] R. Nasirzadeh, A.R. Sabet, Influence of nanoclay reinforced polyurethane foam toward composite sandwich structure behavior under high velocity impact, *J. Cell. Plast.* 52 (3) (2016) 253–275.
- [77] M.H. Pol, G. Liaghat, E. Zamani, A. Ordys, Investigation of the ballistic impact behavior of 2D woven glass/epoxy/nanoclay nanocomposites, *J. Compos. Mater.* 49 (12) (2015) 1449–1460.
- [78] A. Moallemzadeh, S. Sabet, H. Abedini, H. Saghafi, Investigation into high velocity impact response of pre-loaded hybrid nanocomposite structure, *Thin-Walled Struct.* 142 (2019) 405–413.
- [79] J.M. Esfahani, M. Esfandeh, A.R. Sabet, High-velocity impact behavior of glass fiber-reinforced polyester filled with nanoclay, *J. Appl. Polym. Sci.* 125 (S1) (2012) E583–E591.
- [80] A.M. Thayer, Carbon nanotubes by the metric ton, *Chem. Eng. News* 85 (46) (2007) 29–35.
- [81] K. Pandya, K. Akella, M. Joshi, N. Naik, Ballistic impact behavior of carbon nanotube and nanosilica dispersed resin and composites, *J. Appl. Phys.* 112 (11) (2012) 113522.
- [82] Z. Naghizadeh, M. Faezipour, M.H. Pol, G.H. Liaghat, A. Abdolkhani, Improvement in impact resistance performance of glass/epoxy composite through carbon nanotubes and silica nanoparticles, in: *Proceedings of the Institution of Mechanical Engineers, Part L: Journal of Materials: Design and Applications*, vol. 232, 2018, pp. 785–799, 9.
- [83] D. Micheli, A. Vricella, R. Pastore, A. Delfini, A. Giusti, M. Albano, M. Marchetti, F. Moglie, V.M. Primiani, Ballistic and electromagnetic shielding behaviour of multifunctional Kevlar fiber reinforced epoxy composites modified by carbon nanotubes, *Carbon* 104 (2016) 141–156.
- [84] Z. Naghizadeh, M. Faezipour, M. Hossein Pol, G. Liaghat, A. Abdolkhani, High velocity impact response of carbon nanotubes-reinforced composite sandwich panels, *J. Sandw. Struct. Mater.* (2017), 1099636217740816.
- [85] H. Khosravi, R. Eslami-Farsani, High-velocity impact properties of multi-walled carbon nanotubes/E-glass fiber/epoxy anisogrid composite panels, *J. Comput. Appl. Res. Mech. Eng.* (2018).
- [86] H. Khoramshad, H. Alikhani, S. Dariushi, An experimental study on the effect of adding multi-walled carbon nanotubes on high-velocity impact behavior of fiber metal laminates, *Compos. Struct.* 201 (2018) 561–569.
- [87] M. Tehrani, A. Boroujeni, T. Hartman, T. Haugh, S. Case, M. Al-Haik, Mechanical characterization and impact damage assessment of a woven carbon fiber reinforced carbon nanotube–epoxy composite, *Compos. Sci. Technol.* 75 (2013) 42–48.
- [88] U.O. Costa, L.F.C. Nascimento, J.M. Garcia, S.N. Monteiro, F.S.d. Luz, W. A. Pinheiro, F.d.C. Garcia Filho, Effect of graphene oxide coating on natural fiber composite for multilayered ballistic armor, *Polymers* 11 (8) (2019) 1356.
- [89] I.I.M. Priya, B. Vinayagam, Enhancement of bi-axial glass fibre reinforced polymer composite with graphene platelet nanopowder modifies epoxy resin, *Adv. Mech. Eng.* 10 (8) (2018), 1687814018793261.
- [90] V. Alfredsson, M. Keung, A. Monnier, G.D. Stucky, K.K. Unger, F. Schüth, High-resolution transmission electron microscopy of mesoporous MCM-41 type materials, *J. Chem. Soc., Chem. Commun.* (8) (1994) 921–922.
- [91] A. Manero II, J. Gibson, G. Freihofer, J. Gou, S. Raghavan, Evaluating the effect of nano-particle additives in Kevlar® 29 impact resistant composites, *Compos. Sci. Technol.* 116 (2015) 41–49.
- [92] N. Domun, C. Kaboglu, K.R. Paton, J.P. Dear, J. Liu, B.R. Blackman, G. Liaghat, H. Hadavinia, Ballistic impact behaviour of glass fibre reinforced polymer composite with 1D/2D nanomodified epoxy matrices, *Compos. B Eng.* 167 (2019) 497–506.
- [93] D. Toorchi, H. Khosravi, E. Tohidlou, Synergistic effect of nano-ZrO₂/graphene oxide hybrid system on the high-velocity impact behavior and interlaminar shear strength of basalt fiber/epoxy composite, *J. Ind. Textil.* (2019), 1528083719879922.
- [94] J. Gibson, J. McKee, G. Freihofer, S. Raghavan, J. Gou, Enhancement in ballistic performance of composite hard armor through carbon nanotubes, *Int. J. Soc. Netw. Min.* 4 (4) (2013) 212–228.
- [95] H. Fouda, K. Ghith, L. Guo, Enhancement the Armor Shielding Properties of CF/epoxy Composite by Addition Nanoparticles of Magnetic Iron Oxide, *MATEC Web of Conferences*, EDP Sciences, 2017, 01002.
- [96] D.M. Simić, D.B. Stojanović, M. Dimić, K. Mišković, M. Marjanović, Z. Burzić, P. S. Uskoković, A. Zak, R. Tenne, Impact resistant hybrid composites reinforced with inorganic nanoparticles and nanotubes of WS₂, *Compos. B Eng.* 176 (2019) 107222.
- [97] A.F. Ávila, A.S. Neto, H.N. Junior, Hybrid nanocomposites for mid-range ballistic protection, *Int. J. Impact Eng.* 38 (8–9) (2011) 669–676.
- [98] G. Balaganesan, M. Pushparaja, R. Velmurugan, N. Gupta, Impact loading on nanocomposites in thermal environment, *Procedia IUTAM* 23 (2017) 210–219.
- [99] E.T. Thostenson, C. Li, T.-W. Chou, Nanocomposites in context, *Compos. Sci. Technol.* 65 (3–4) (2005) 491–516.
- [100] S. Pavlidou, C. Papispyrides, A review on polymer-layered silicate nanocomposites, *Prog. Polym. Sci.* 33 (12) (2008) 1119–1198.
- [101] X.-L. Xie, Y.-W. Mai, X.-P. Zhou, Dispersion and alignment of carbon nanotubes in polymer matrix: a review, *Mater. Sci. Eng. R Rep.* 49 (4) (2005) 89–112.
- [102] L. Sun, R.F. Gibson, F. Gordanejad, J. Suhr, Energy absorption capability of nanocomposites: a review, *Compos. Sci. Technol.* 69 (14) (2009) 2392–2409.
- [103] J. Viana, Polymeric materials for impact and energy dissipation, *Plastics, Rubber and Composites* 35 (6–7) (2006) 260–267.
- [104] H.-Y. Liu, G.-T. Wang, Y.-W. Mai, Y. Zeng, On fracture toughness of nano-particle modified epoxy, *Composites Part B* 42 (8) (2011) 2170–2175.
- [105] I. Dubnikova, S. Berezina, A. Antonov, Effect of rigid particle size on the toughness of filled polypropylene, *J. Appl. Polym. Sci.* 94 (5) (2004) 1917–1926.
- [106] W. Wöhlehen, J. Mielke, A. Bianchin, A. Ghanem, H. Freiburger, H. Rauscher, M. Gemeinert, V.-D. Hodoroaba, Reliable nanomaterial classification of powders using the volume-specific surface area method, *J. Nanoparticle Res.* 19 (2) (2017) 61.
- [107] D.A. Almasri, T. Rhadfi, M.A. Atieh, G. McKay, S. Ahzi, High performance hydroxyiron modified montmorillonite nanoclay adsorbent for arsenite removal, *Chem. Eng. J.* 335 (2018) 1–12.
- [108] A. Peigney, C. Laurent, E. Flahaut, R. Bacsa, A. Rousset, Specific surface area of carbon nanotubes and bundles of carbon nanotubes, *Carbon* 39 (4) (2001) 507–514.
- [109] Y. Qian, I.M. Ismail, A. Stein, Ultralight, high-surface-area, multifunctional graphene-based aerogels from self-assembly of graphene oxide and resol, *Carbon* 68 (2014) 221–231.
- [110] C.-K. Chu, Y.-L. Chen, Ballistic-proof Effects of Various Woven Constructions, *Fibres & Textiles in Eastern Europe*, 2010.